THE APPLICATION OF DIRECT-CURRENT RESISTIVITY PROSPECTING METHODS TO ICE MASSES

by

JOHN PHILLIPS GREENHOUSE

B.Sc., The University of British Columbia, 1960.

A THESIS SUBMITTED IN PARTIAL FULFILMENT OF

THE REQUIREMENTS FOR THE DEGREE OF

MASTER OF SCIENCE

in the Department

of

PHYSICS

We accept this thesis as conforming to the

required standard

THE UNIVERSITY OF BRITISH COLUMBIA

February, 1963.

In presenting this thesis in partial fulfilment of the requirements for an advanced degree at the University of British Columbia, I agree that the Library shall make it freely available for reference and study. I further agree that permission for extensive copying of this thesis for scholarly purposes may be granted by the Head of my Department or by his representatives. It is understood that copying or publication of this thesis for financial gain shall not be allowed without my written permission.

Department of Physics

The University of British Columbia,
Vancouver 8, Canada.

Date 20/2/63.

ABSTRACT

Direct-current resistivity prospecting methods have been used but rarely in the past in physical investigations of ice-caps and glaciers. However these methods have the advantage of using light-weight and inexpensive equipment that is simple to operate. As part of the geophysical program of the Arctic Institute of North America's Devon Island Expedition, resistivity measurements were made in the accumulation and ablation zones of an ice-cap and on an adjoining glacier during the summers of 1961 and 1962.

Depths of ice ranging from 50 to 750 meters were measured on the Sverdrup Glacier. Depth soundings on the ice-cap were not very successful owing primarily to insufficient power. However, some indication of the depth and composition of the firn was obtained. Ice resistivities were for the most part in the range from 4.10^4 to 10^5 ohm-meters, as compared with values of several megohm-meters found for temperate glaciers in lower latitudes. Variations of ice resistivities as a function of other physical properties were investigated.

TABLE OF CONTENTS

TABLE OF CONTENTS (continued)

LIST OF FIGURES

LIST OF TABLES

Table

PREFACE

The purpose of this study is to describe and evaluate the use of direct-current resistivity prospecting methods in investigations of the depth and physical properties of glaciers and ice sheets. Particular attention is paid to the results of field work carried out with the Arctic Institute of North America's Devon Island Expedition during two summers. The Devon Island program of resistivity work is believed to be the most extensive of its type to date, and it is felt that an assessment of this method as a glaciological tool is now of value. The conduction mechanisms of ice are extremely complex and they are not dealt with here in any detail. However, the resistivity difference found to exist between Arctic ice sheets and those of continental America, Asia, and Europe is described, and the factors involved are discussed. Not all the possibilities of direct-current methods on glacial ice have been explored, nor are all the results obtained completely understood. The present study will discuss the applications investigated to date, suggest others that appear promising, and give a detailed description of measuring techniques.

I wish to express my thanks to the Arctic Institute of North America, who sponsored the field work; to the Institute of Earth Sciences, University of B.C., which lent equipment; to Dr. J.C. Savage for his suggestions and criticisms; and to Mr. R.H. Hyndman and Lt. R.A. Tansey for their assistance in carrying out the field work.

Dr. K. Vogtli, who initiated the resistivity work on Devon Island, has made many suggestions concerning the work for which I am most grateful. I have taken the liberty of including four of his curves in the present study.

In particular, I should like to express my sincerest thanks to Dr. J.A. Jacobs who has given me encouragement and assistance in every stage of the work that preceded this thesis.

I. INTRODUCTION

Although by no means a new idea, the application of resistivity techniques to ice masses has been infrequently practised. Probably the fact that pure ice is highly insulating at low frequencies dissuaded glaciologists originally from attempting direct-current measurements. However glacial ice, taken as a whole, has electrical properties that differ considerably from those of pure ice. In addition, the properties of ice of most interest to glaciologists, such as temperature, crystal structure and density, are important parameters of the conductivity in any material. These factors alone render an investigation worthwhile.

Previous applications of resistivity methods to ice masses.

The earliest obtainable reference, an abstract of a Russian report describing field work in 1939, contains the following remarks (Mikhailov, 1939, SIPRE abstract).

'The determination of the thickness of glacier ice by seismic reflection is considered unreliable because secondary waves at high altitudes are difficult to distinguish in thin glaciers. The measurement of specific resistance of glacier ice by electrical resistance methods is believed to be reliable. A diagram was made from data collected on Mt. Elbrus* expressing specific resistance as a function of the distance between electrodes, the length of the circuit, the difference in potentials of the electrodes, and the current. The resistivity of the upper layer of the glacier was 3 megohm-meters, ...'

In 1956 and 1957 a team from the Laboratoire de Géophysique Appliquée et Expéditions Polaires Françaises made two trips to

* S.W. Russia

central European glaciers to experiment with resistivity measurements on ice, using both natural earth currents and current externally applied. On the Grand Glacier d'Aletsch they determined a mean resistivity of the order of 10 megohm-meters for the glacier ice (Lefeure et al, 1957). On the Glacier de Saint Sorlin in the French Alps an ice depth of 80 meters was recorded, the ice having a resistivity of about 80 megohm-meters (Queille - Lefeure et al, 1959).

At the Twelfth General Assembly of the International Union of Geodesy and Geophysics at Helsinki in 1960, B.A. Borovinski (1960) presented a paper describing work done on the glaciers of Kazakhstan as part of the International Geophysical Year program. Borovinski mentions the advantages of weight and size of resistivity equipment over seismic gear, and claims that electrical methods can be successfully applied to the following problems:

(i) Determination of ice thickness.

(ii) Measurement of the velocity of "inner ice layers".

(iii) Determination of the elastic constants of ice at depth.

(iv) Determination of the shape of a glacier bed.

(v) The study of moraines.

(vi) "To ascertain sections of increased thawing of the ice down the glacier's surface."

Few details are given to substantiate these somewhat unreserved statements. It is probable however that resistivity methods on ice have been extensively investigated in the Soviet Union, although English abstracts are not available.

In 1959, G.V. Keller and F.C. Frischknecht (1960) of the United States Geological Survey experimented with electrical and electro-magnetic methods on the Athabaska Glacier in Alberta. Using a pulsed direct-current technique to determine simultaneously the apparent resistivity and the dielectric constant they identified two layers: a surface layer with resistivity varying from 0.07 to 1.8 megohm-meters and a second layer extending to bedrock with a resistivity of 10 to 20 megohm-meters.

During the past few years the Swiss Post - Telegraphen - und Telephonverweltung (P.T.T.) has undertaken an investigation of the electrical properties of glacial ice in connection with the laying of power lines across and through glaciers. Glacial ice resistivities encountered ranged from 10 to 60 megohm-meters (Vöglti, 1957).

Following reports that the resistivity of ice on the Greenland ice-cap was smaller by two to three orders of magnitude than that of continental European, Asian, and American glaciers, Dr. K. Vögtli of the Swiss P.T.T. spent two months in the summer of 1961 on Devon Island in the eastern Canadian Arctic. In addition to determining that the ice there has a resistivity similar to that reported in Greenland, Dr. Vögtli carried out a resistivity survey of a glacier on the north coast, measuring depths and resistivities from source to snout. In isolated cases, regions of megohm-meter resistivity were encountered and some of the "dead" tributary glaciers (i.e. glaciers that no longer joined the ice-cap at their heads) displayed

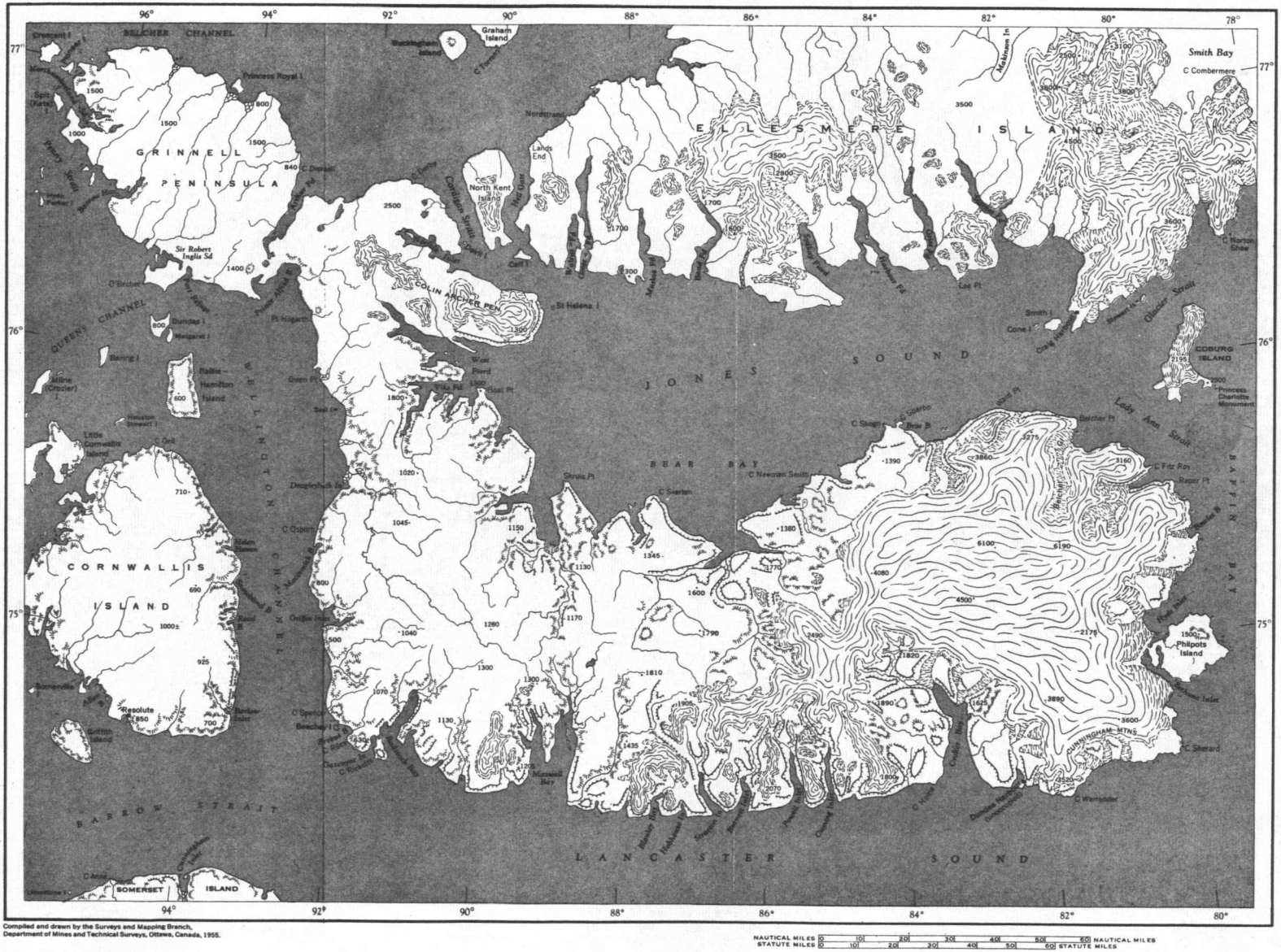

Figure 1. Location Map - Devon Island.

intermediate values of resistivity.

The resistivity work carried out on Devon Island during the summer of 1962 extended these studies to the ice-cap. Measurements were taken both in the accumulation zone and the ablation zone, and it was hoped that ice thicknesses could be obtained to complement the gravity survey carried out simultaneously.

Electrical properties of snow and ice.

The theory of charge conduction in ice crystals is as yet incomplete. Eigen and deMaeyer (1958) refer to ice as a "protonic semi-conductor" since the hydrogen-bonded system can exhibit excess and defect proton charge transport. The mobility of the proton exceeds that of any other ion in the lattice by several orders of magnitude and approaches closely the electronic mobilities in metals and certain semi-conductors. The transition from water to ice is accompanied on the one hand by an increased proton mobility and on the other by a decreased proton concentration, leaving the conductivities of the two phases much the same. The uncertain aspect of the theory is the process determining the rate of the proton's passage through the hydrogen-bonded molecular chains.

Impurities present in the water are concentrated on freezing either between the plates of the crystal or around the crystal walls. The intersticial material can be expected to contribute electronic and ionic conduction, and the conductivity of the impure ice is much increased (Mantis, 1951, p.39).

The dielectric properties of ice and snow have been frequently

studied and an idea of their direct-current behaviour may be obtained by extrapolating the results at very low frequencies. If the complex dielectric constant of pure ice, given by

$$\epsilon^* = \epsilon' - i\epsilon'' = \frac{C_s}{C_a} - i\frac{G}{\omega C_a} \qquad \text{(m.k.s. units)}$$

where C_s = Capacitance of test capacitor with sample inserted.

C_a = Capacitance of test capacitor without sample.

G = Conductance of test capacitor.

ω = Angular frequency = $2\pi f$

$i = \sqrt{-1}$

is plotted on an Argand diagram (fig. 2) it is seen that the conductivity at zero frequency is effectively zero. For impure ice the low frequency section of the curve deviates markedly from the semi-circle. Auty and Cole (1952) found a resistivity of nearly 10^8 ohm-meters at -0.10°C and a frequency of 100 cycles per second. The value continued to decrease with frequency. Similar tests by Watt and Maxwell (1960) on ice from the Athabaska Glacier showed a resistivity that approached constant values between 3.10^5 and 2.10^6 ohm-meters at -0.10°C as the frequency went below 200 cycles per second. Below 200 cycles per second the conductivity of glacier ice increased with temperature.

R. Siksna (1957) has studied the electrical conduction of ice crystals both by observing the rate of discharge of a capacitor through a sample and by placing the crystal directly in a

Figure 2. Dielectric Properties of Pure and Glacial Ice.

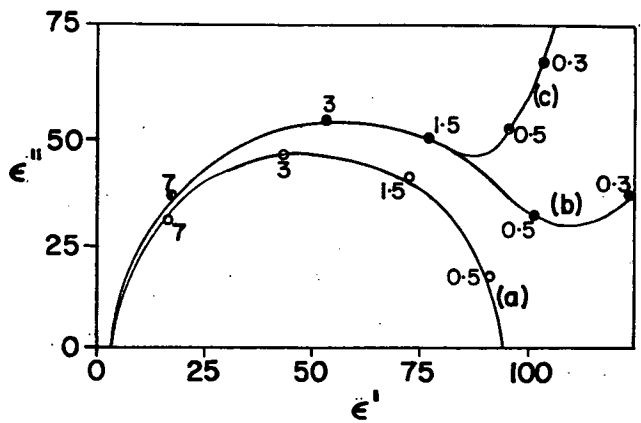

(i) Complex dielectric constants of ice samples at -10.8°C. (a) Pure ice. (b) and (c) Samples with electrode polarization arising from d.c. conductance. Numbers beside points are frequencies in kc/s. (After Auty and Cole, 1952, fig. 2).

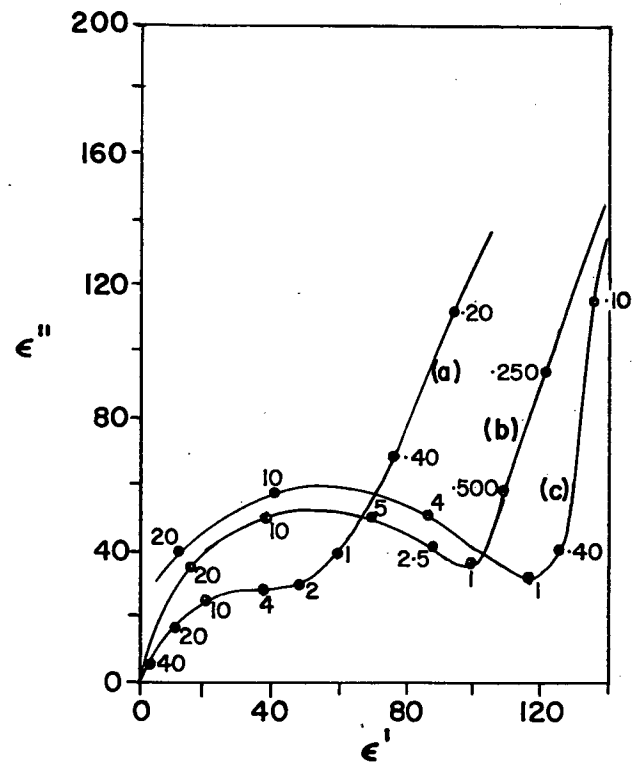

(ii) Complex dielectric constants of glacier ice at 0°C. (a), (b) and (c) are curves for various electrode configurations at various locations. (After Watt and Maxwell, 1960, fig. 10).

circuit through which current was flowing. He found the conductivity to be dependent on:

(i) Temperature. The conductivity, for a given applied potential, could increase by several hundred percent between the temperatures of -25.5°C and -4.5°C.

(ii) The direction of current with respect to the optic axis. Variations in this case seemed to be largely dependent on the electrical history (see iv).

(iii) The applied potential. For a given set of conditions, the conductivity decreased with increasing potential.

(iv) Electrical history. The conductivity of a sample underwent a marked decrease after the sample had been electrically stressed over a period of time. The resistivity of ice at -10°C increased by a factor of 800 when the sample was connected to one terminal of a 135 volt battery for a three day period. Reversing the measuring current restored the conductivity to its original order of magnitude. Siksna attributes the current decrease in the circuit to a piling up of the available carriers at the electrodes. His observation is of interest since a similar polarization effect was observed in the present field investigations, when the effective resistance of the glacial ice in the circuit increased markedly with time when a current was passed (see Table II).

A polycrystalline sample of ice can be expected to exhibit polarization at internal surfaces such as cracks, air bubbles, and intergranular boundaries (Mantis, 1951, p. 39). Thus the

conductivity of a sample will depend both on its density and on the size and orientation of its grains. This assumes that the temperature is sufficiently low that conduction cannot occur through concentrated solutions of impurities along the granular interfaces. This assumption is certainly valid for the Arctic ice masses to be discussed, especially in view of the melt sample conductivities given in Table I.

Snow is composed of ice crystals and air spaces: its dielectric properties are determined by the volume ratio of the two media and the overall structure. There exist in nature an almost limitless number of possible structures, combinations of grain size and density. In addition the snow may contain free water which will greatly alter the electrical properties. The dielectric properties of dry snow, however, depend predominantly on the density and on the dielectric properties of the ice-crystals (for discussion see Kuroiwa, 1954).

The low resistivity of Arctic ice sheets.

The ice resistivities encountered on Devon Island differed by two to three orders of magnitude from those of temperate glaciers previously investigated. The pertinent factors to be considered are as follows:

(i) Temperature. The fact that the colder ice is a much better conductor than the comparatively warm ice rules out temperature as a possible cause.

(ii) Impurity content. In the absence of proper chemical analysis, the conductivities of melt water samples from various

TABLE I

Resistivity of Water Samples

Location	Resistivity (ohm-meters) at 0°C unless otherwise indicated.
1. Sea Ice.	0.20
2. Lake water (Devon Island).	59
3. Melt stream (Sverdrup Glacier).	203
4. Melt stream (Athabaska Glacier). (Keller and Frischknecht, 1960, p. 447)	650
5. Snow (Sverdrup Glacier).	1300
6. Snow (Devon Island Ice-cap)	2510 2270 4020 2780 (1.1°C) 2000 (3.5°C) 2080 (5.0°C)
7. Ice (Devon Ice-cap)	2370 3920 (4.0°C)
8. Firn and old snow (Accumulation zone)	
Surface	6050 (2.8°C)
At 1.5 meters	9890
At 8 meters	4840
9. Distilled water.	5350

locations are compared in Table I. The evidence is very limited and the samples are of necessity taken from the surface. Moreover the effects of impurities on the conduction mechanisms of water and ice need not be of the same order of magnitude. It can be seen that resistivities of samples from the Sverdrup and Athabaska Glaciers are very similar; of greater significance however is the comparison of the resistivities of ice-cap samples and distilled water. Despite considerable variation from sample to sample in a given area, this close correspondence would indicate that the impurity content of the Arctic ice is very low. Possibly small quantities of a particular impurity in the crystal lattice are responsible for the observed resistivity contrast; otherwise the available evidence does not point to impurities as the origin of the difference.

The conductivities of the Devon Island samples were measured with a Philips Conductivity Measuring Bridge (PR 9500).

(iii) Crystal Structure. It has been suggested that the resistivity of ice samples could depend on the size and orientation of the grains, which in turn can be related to age, temperature, and internal stress. One method of determining the importance of structural differences is to measure the resistivity of the unconsolidated firn in the accumulation zones of the ice masses concerned. If the resistivity difference still exists (differences in firn temperatures being taken into account) then it must be due to the properties of the individual ice crystals; if it no longer exists then structural differences are probably the cause of the anomaly. Firn resistivities have been measured

on Devon Island but as far as is known no such data is available for the temperate glaciers. The resistivity of snow has been measured in various localities by Roman (1936), Shimada (1954), Lee (1936), and Vögtli (1957), but since the temperatures and snow structures are not consistently described there is no basis for comparing the results.

A second method of determining the importance of crystal structure is to measure the resistivity of refrozen melt samples which have recrystallized under different conditions of temperature and pressure than the original ice. The results of such measurements being made by Vögtli are not yet available. Similar information could be obtained from measurements on refrozen melt lakes on the ice-cap and glacier surfaces.

II. THEORY OF THE RESISTIVITY METHOD

Solution of Laplace's equation.

Direct-current flow from a source in a homogeneous isotropic conducting medium is analogous to the flow of an incompressible fluid; the amount flowing into a closed surface per unit time must equal that flowing out. Expressed mathematically,

$$\nabla \cdot \vec{i} = 0$$ (where $\vec{i}$ is the instantaneous current density)

Since $\vec{i}$ at any point can be written

$$\vec{i} = -\frac{1}{\rho} \nabla V$$ (where V is the potential and ρ is the resistivity of the medium.)

the potential function satisfies Laplace's equation

$$\nabla^2 V = 0$$

If a point source of current is considered to be situated at the interface between a semi-infinite homogeneous and isotropic conducting medium and a medium of infinite resistance, the potential field is spherically symmetrical in the conducting half space and satisfies the equation

$$\frac{d^2V}{dr^2} + \frac{2}{r}\frac{dV}{dr} = 0$$ (where r is the radial coordinate.)

whence $V = +\frac{S}{r} + C$

where S and C are constants. These constants may be evaluated from the conditions that the potential is zero at $r = \infty$ and the total current passing through a hemisphere of radius r must equal the source strength I. It is found that

$$C = 0 \qquad S = \frac{I\rho}{2\pi}$$ (I may be positive or negative)

Hence $$V(r) = \frac{I\rho}{2\pi r}$$

or $$\rho = 2\pi r \frac{V(r)}{I} \qquad (I)$$

Since in general the medium will not be isotropic or macroscopically homogeneous, this quantity is called the apparent resistivity and written ρ_{app}.

The problem of finding the potential field of a point source in a medium composed of two or more homogeneous isotropic horizontal layers involves satisfying the boundary conditions at each interface:

$$V_1 = V_2$$

$$\frac{1}{\rho_1}\frac{\partial V_1}{\partial z} = \frac{1}{\rho_2}\frac{\partial V_2}{\partial z} \qquad (II)$$

where z is the vertical co-ordinate.
Subscripts 1 and 2 refer to upper and lower layers.

This is done by using the method of images or by direct solution of Laplace's equation under these conditions. The former method is useful in simple horizontal structures but can be applied only in certain cases to structures with dipping beds (Maeda, 1955). Using separation of variables in a cylindrical co-ordinate system and applying the conditions (II) at each interface, Stefanesco et al (1930) derived an expression for the apparent resistivity of the medium in terms of the potential field and the total current. From this result, standard curves are derived for a number of combinations of layer depths and

resistivities, giving apparent resistivity as a function of electrode spacing.

Electrode configurations.

The field work to be described makes use of the electrode configurations of Schlumberger and of Wenner. These are shown schematically in figure 3. The expression for ρ_{app} in each case is obtained by superimposing the potential fields of the current electrodes according to (I). Standard curves are available for the Schlumberger (La Compagnie Générale de Géophysique, 1955) and Wenner (Mooney and Wetzel, 1956, or Vögtli, No. 14104, 1957) configurations. Two and three layer standard curves (Schlumberger) are given in the appendix. Figure 3(c) shows a useful variation of the Wenner configuration. It can easily be shown that an interchange of the current and potential electrodes has no effect on the measured apparent resistivity. In addition, the configurations CPPC, CPCP, CCPP, and their reciprocals, can be shown to yield apparent resistivities ρ^{α}_{app}, ρ^{β}_{app}, and ρ^{γ}_{app} respectively that satisfy the relationship

$$3\,\rho^{\alpha}_{app} = \rho^{\gamma}_{app} + 2\,\rho^{\beta}_{app} \qquad \text{(III)}$$

This relationship provides a useful check on current losses in the equipment and cable.

Current penetration in a two-layer structure.

The effect produced by a subsurface feature on the surface potential field is proportional to the fraction of the total current flowing through it. Muskat and Evinger (1941) have

(a) Schlumberger Configuration.

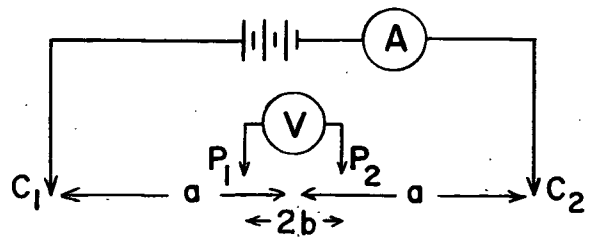

$$\rho_{app} \doteq \pi \frac{a^2}{2b} \frac{\Delta V}{I} \quad \text{for } b \leq \frac{1}{6} a$$

(b) Wenner Configuration.

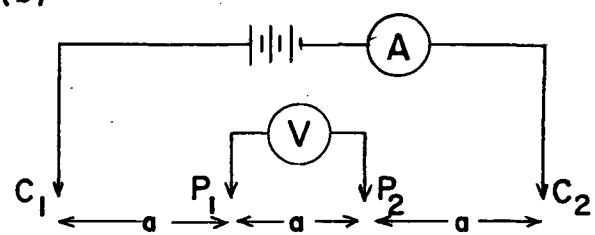

$$\rho_{app} = 2\pi a \frac{\Delta V}{I}$$

(c) Variations on the Wenner configuration. (After Carpenter, 1955, Table 1).

$$3\rho_{app}^{\alpha} = \rho_{app}^{\gamma} + 2\rho_{app}^{\beta}$$

α

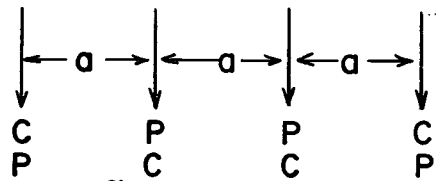

$$\rho_{app}^{\alpha} = 2\pi a \left(\frac{\Delta V}{I}\right)^{\alpha}$$

β

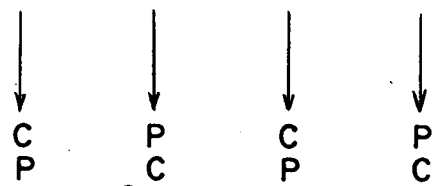

$$\rho_{app}^{\beta} = 3\pi a \left(\frac{\Delta V}{I}\right)^{\beta}$$

γ

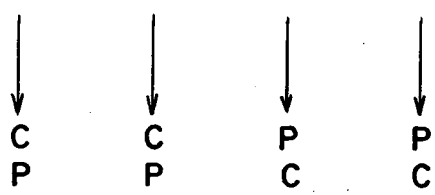

$$\rho_{app}^{\gamma} = 6\pi a \left(\frac{\Delta V}{I}\right)^{\gamma}$$

Figure 3. Electrode Configurations.

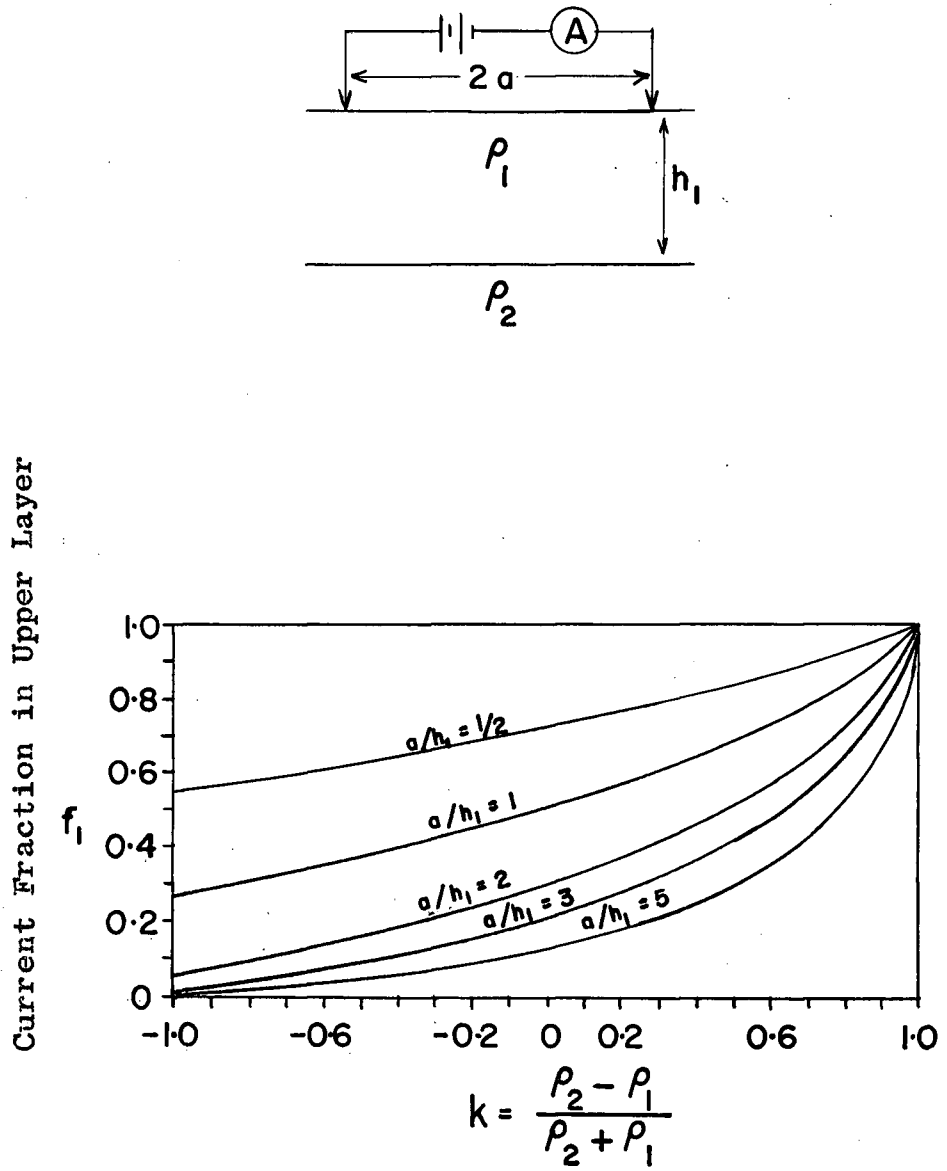

Figure 4. Current Penetration in a Two-layer Structure. (After Muskat and Evinger, 1941, fig. 4)

plotted the fraction f of current flowing in various resistivity combinations of two and three-layer horizontal structures. Figure 4 shows the current fraction flowing in the upper layer of a two-layer model. This is an important concept for qualitative interpretation.

III. APPARATUS AND MEASUREMENTS

The resistivity equipment used on Devon Island, including 6500 meters of cable, did not exceed 130 pounds in weight, and with the possible exception of the instrument case, contained no bulky components. The principal articles were: the instruments and case (25 lbs.); cable (65 lbs.); electrodes (15 lbs.); marker flags (5 lbs.); and 3 radios (20 lbs.). Measurements with a maximum current electrode separation of 1300 meters required only 60 pounds of equipment, a load easily distributed between two men.

Instruments and measuring circuit.

The measuring circuit is shown in figure 5(a). Any one of the central terminals of the four switches, SW1, SW3, SW4 and SW5 can be connected to any one of the electrodes attached to SK1 to SK5*. The current flow is adjusted by means of a potential divider set across a variable number (SW2) of series-connected $67\frac{1}{2}$ volt dry cells. The value of R is chosen to give linear performance over the range of the potential divider. The voltmeter (V) is a Keithley model 600A Electrometer, an instrument whose high input impedance (10^{14} ohms) prevents distortion of the measured field. The current flow is measured by a Simpson model 269 multimeter (A) capable of reading 16 microamperes full scale. SW6 is an off-on switch for the

*A fifth electrode is used in the Lee Partition Method a variation of the Wenner Method used for determining the slope of the interface in a two-layer case.

Figure 5.

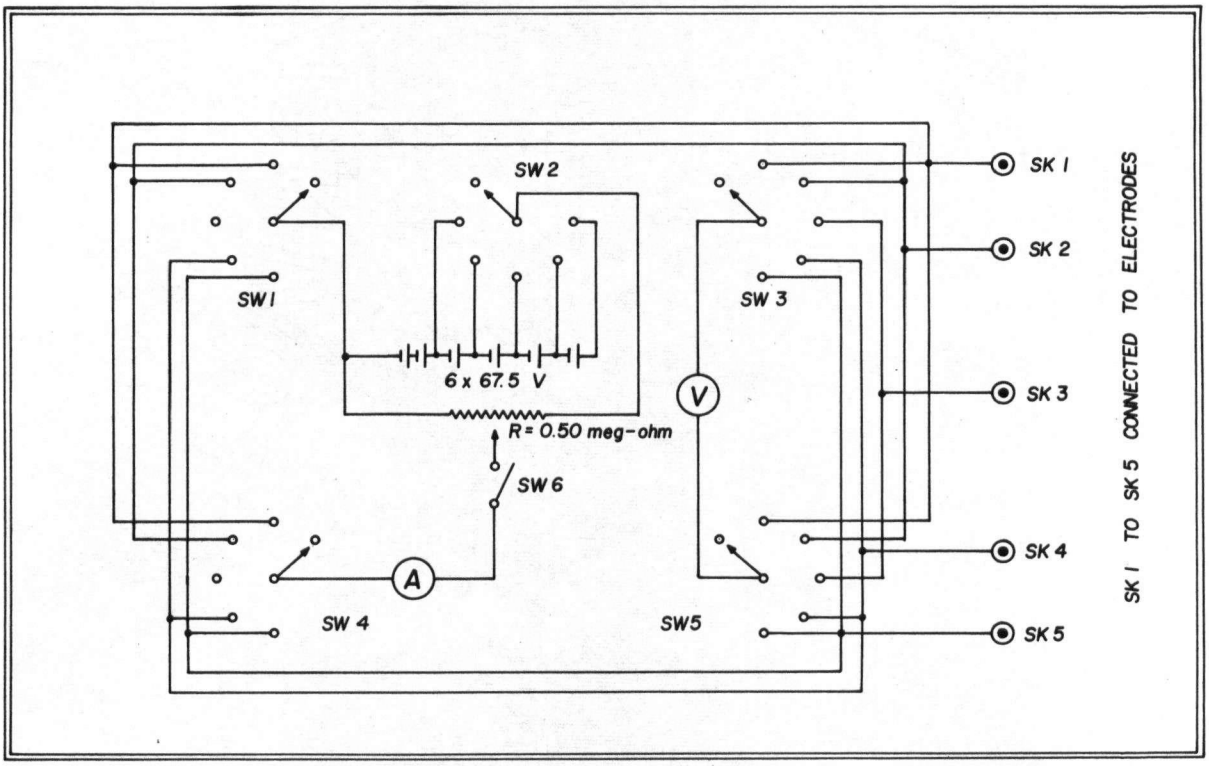

(a) The Measuring Circuit.

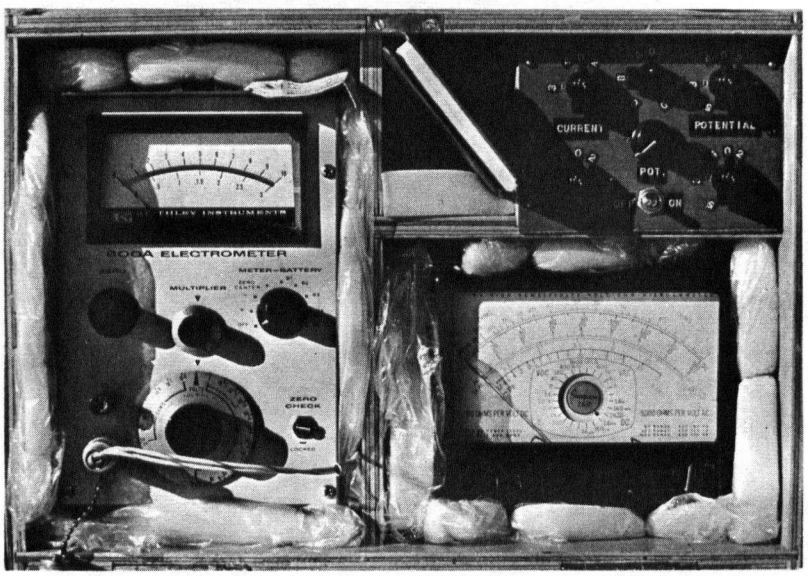

(b) Instruments and Case.

current circuit. Batteries, instruments, and wiring are fitted into a canvas covered wooden case (fig. 5(b)). The two instruments, both easily removable, are surrounded by half inch slabs of polyethlene foam to lessen vibration and to isolate them electrically. The electrode cables are attached to the back of the case by means of Cannon type 12S connectors.

Electrodes and cable.

Ideally the current electrode is a point source. In practice this is closely approximated by using a pointed metal stake. For a given imposed voltage and electrode spacing the current is critically dependent on the contact resistance at the electrode. If the surface is ice the stake is placed in a crack or water-filled hole and "salted" to improve the contact. If the surface is snow the area around the stake is thoroughly packed and a brine solution poured over the stake. With large electrode separations the contact area can be increased by using several stakes connected in parallel and arranged in a circle. From the expression for the potential field of each stake (I) it can be seen that at separations of the potential and current electrodes large compared with the diameter of the circle the resultant field is essentially that of a point source. Frequently a spade or a wire mesh is used as a current electrode at large separations.

The potential electrodes consist of copper rods immersed in a copper-sulphate solution, the whole being enclosed in a clay jar with a porous lower half. The jar is 6 inches high with

inside diameter 2½ inches, and the rod enters through a neoprene stopper. This arrangement ensures that the contact potentials of the two electrodes are similar to within a few millivolts; thus the voltmeter will not be thrown off-scale on the lower voltage ranges. Ideally the solutions are saturated, and at the same temperature; in practice it is sufficient to keep the concentrations equal.

The cable used on Devon Island consisted of six strands of copper and one of steel insulated by a single layer of polyethlene to give an overall diameter of 1.8 mm. The cable was wound on ten hand-reels each carrying 650 meters. One reel with cable weighed 6.5 pounds.

Reading procedure.

While it is possible for one man to run the equipment, three men (a central operator and a man for each side) are necessary for efficient operation. Procedure can be itemized as follows:

(i) Using a fabric measuring tape (50 or 30 meters in length depending on the wind) the electrode distances are measured from a chosen center. The distances "a" are chosen so as to give an even spacing of points on the logarithmic scale on which the standard curves are plotted. This set of measured distances is termed a "profile".

(ii) The cable is reeled out from the center, two reels being joined when necessary. At each point of the profile an electrode is inserted and readings taken. At separations of over 500 meters, communication between the central and outlying

personnel is achieved by radio or by means of ammeters adjacent to, and in series with, the current electrodes. This latter method, besides being generally more reliable than radio, acts as a check on current losses along the cable. The man at the electrode can read the current directly and adjust his electrode if the flow is insufficient. Signals are given by interrupting the current flow.

(iii) Once the electrodes are in place, the recording procedure is as follows:

(a) the current is adjusted to a convenient value, large enough to produce an appreciable potential ΔV but not so large as to be a significant drain on the batteries.

(b) The voltmeter is connected on a suitable range and its reading V_1 and the current I recorded.

(c) The batteries are disconnected from the circuit and the new voltmeter reading V_2 (the background potential) recorded. Then

$$V_2 - V_1 = \Delta V$$

This method of measuring ΔV is considered preferable to the often used technique of setting V_2 equal to zero by cancelling the background potential with a counter e.m.f. The background can drift considerably and it is convenient to average by eye several successive measurements as described in (b) and (c).

(d) The current flow is reversed and steps (b) and (c) repeated. While it would be useful to repeat (a) to (d) using a different value of current it is advisable to take all readings with the same needle position of the ammeter to avoid errors due

to the non-linearity of the scale.

(e) The values ΔV and I are inserted in the appropriate equation and ρ_{app} computed and plotted as a function of "a" on log-log paper. The experimental curve is then compared with standard curves.

When time permitted two profiles were measured at right angles from the same center to check the results and the isotropy of the ice.

Limits of accuracy.

Ideally reading errors should not contribute more than 4 percent but under difficult conditions this factor may be exceeded. Errors in distance measurements are negligible. Otherwise the accuracy of depths and resistivities depends entirely on the fit obtained with the standard curves. Standard curves can be computed for any arrangement of electrodes and any combination of the measured quantities using the tables prepared by Mooney and Wetzel (1956), but generally the spread of the points through which the experimental curve is drawn is such that the combinations available in published standard curves are adequate. A single profile cannot be expected to give ice depth to better than 25 percent. However, if several such profiles are read and if the parameters such as ice and bedrock resistivities are known, accuracies of 10 to 15 percent are possible.

Relative advantages of the Schlumberger and Wenner methods in this application.

For a given current I and spacing "a" the method of Wenner

has the advantage of yielding a value ΔV approximately twice that given by the method of Schlumberger. In addition, with the electrodes in place three interrelated apparent resistivities can be measured by switching leads as explained previously. However, the Wenner arrangement requires almost twice the amount of cable to probe the same depth and both the potential and current electrodes must be moved considerable distances between readings. With the Schlumberger configuration, the potential electrodes can be quickly manipulated by the central operator. In this particular application the method of Schlumberger is more efficient; occasional Wenner readings should be taken as a check on results.

Common difficulties arising in obtaining the measurements.

These are listed in Table 3.

Evaluation of equipment.

While the equipment shown in figure 5 functioned well on the whole, the case was not always successful in insulating components. Despite the precautions taken to keep batteries, instruments, and connections dry, it became virtually impossible to eliminate stray currents when riming and freezing rain conditions prevailed. On such occasions it was necessary to remove the components from the case and suspend them above the surface, if necessary inside a tent.

A persistent difficulty occurred with large potential electrode separations when reversing the voltmeter leads caused

TABLE II

Common Difficulties Arising in Obtaining the Measurements

SYMPTOMS	PROBABLE CAUSES	REMEDY
1. Initial current drops rapidly; cannot be held at steady value.	(i) Polarization at the current electrodes and in cracks and bubbles throughout ice.	(i) Reverse direction of current.
	(ii) Contact resistance at electrode rapidly increasing due probably to freezing of applied solution.	(ii) Apply more salt to the electrodes.
2. Voltmeter cannot be kept on scale in desired range.	(i) Unequal concentration of solutions in pots.	(i) Re-mix the solution.
	(ii) One or both pots no longer porous.	(ii) Clean pots.
	(iii) Earth currents.	(iii) Wait for quieter conditions.
	(iv) Solution freezing. Potential between liquid and solid phases may be as much as 100 millivolts.	(iv) Keep heated supply of solution available.
3. Apparent resistivity anonamously high.	Stray currents influencing voltmeter.	Check insulation and connections.
4. Apparent resistivity anonamously low.	Current flow short-circuited.	Check connections. Watch for current electrodes too close to melt streams.

the value of ΔV to vary by several millivolts. The effect occurred whether or not there was current flowing in the ground; however, it occurred only if the current cables were laid out. Presumably a stray current was biasing the voltmeter, but its origin could not be determined.

IV. RESULTS

The Devon Island ice-cap is approximately 15,000 square kilometers in area and overlies a plateau consisting of exposed Pre-Cambrian rocks to the north, east and southeast, and Paleozoic sediments to the south and west. Figure 6 is a topographic map of the ice-cap, showing the area with which the Devon Island Expedition was concerned.

Interpretation of both the resistivity and gravity surveys is hampered by the present lack of seismic soundings on the glacier and ice-cap. It is thought that a limited number of seismic measurements will be made in the spring of 1963.

Subdivision of the resistivity curves.

For the purpose of discussion, four characteristic features of the resistivity curve can be defined. Any or all of these features may be present in a given curve.

(i) The surface effect. This is seen as a positive or negative slope at the commencement of the curve which may extend over the first two to three meters of the abscissa "a". It is produced either by surface melting, or by a thin layer of snow overlying the ice surface.

(ii) The shallow subsurface effect. This takes the form of a plateau or convex segment which may extend over the first few tens of meters of the abscissa. In the accumulation zone this feature is very pronounced and is referred to as the firn curve. It is often present too in the ablation zone, appearing as a high

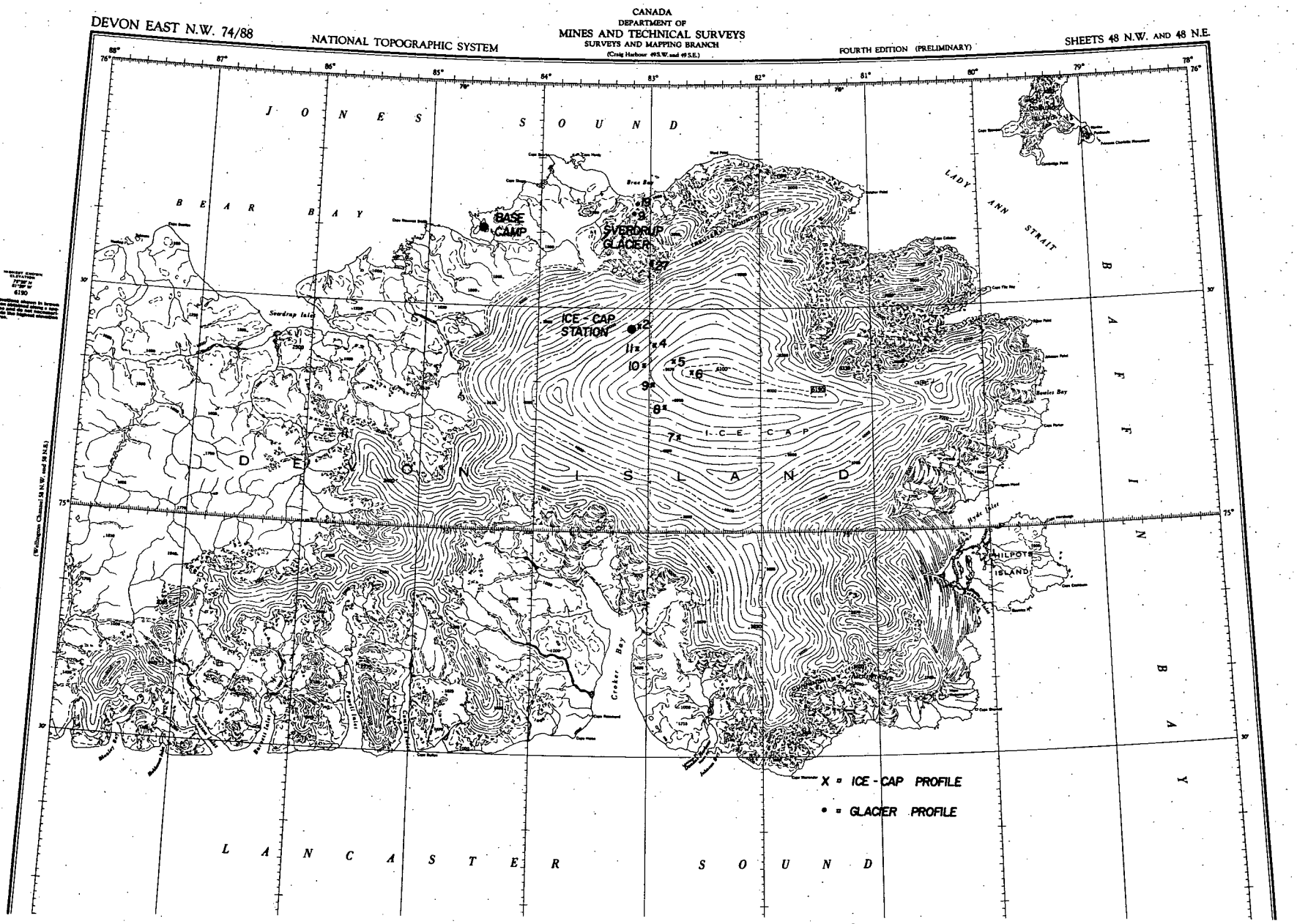

Figure 6. The Devon Island Ice-cap. Scale approx. 12 km. to 1 cm.

resistivity layer in the top ten to twenty meters of ice.

(iii) The bulk resistivity. This denotes the portion of the curve between the shallow subsurface effect and the bedrock effect (iv). The apparent resistivity of this section can be described as the mean resistivity of the ice.

(iv) The bedrock effect. This segment terminates the curve and has an upward or downward slope depending on the resistivity of the bedrock.

1961.

The geophysical program in 1961 was confined almost entirely to the Sverdrup Glacier. This work will be described in Dr. K. Vögtli's report to the Arctic Institute of North America for that season. Figures 7 and 8 show three resistivity curves from the glacier.

Figure 7 shows ideal interpretative conditions where the shallow subsurface effect is scarcely evident. In Figure 8 is shown an example of a very large shallow subsurface effect. The profiles plotted at each point are indicated on the figure by a double ended arrow marked with the direction (if pertinent) and the symbol used in plotting results (if two or more profiles were measured). An S signifies the Schlumberger configuration, a W that of Wenner. Standard curves are shown when considered necessary. The interpretation given on the figures assumes that all features of the curve arise from horizontal stratification. It should be remembered that the surface effect in particular may stem from near surface inhomogeneities, and a "layer" interpre-

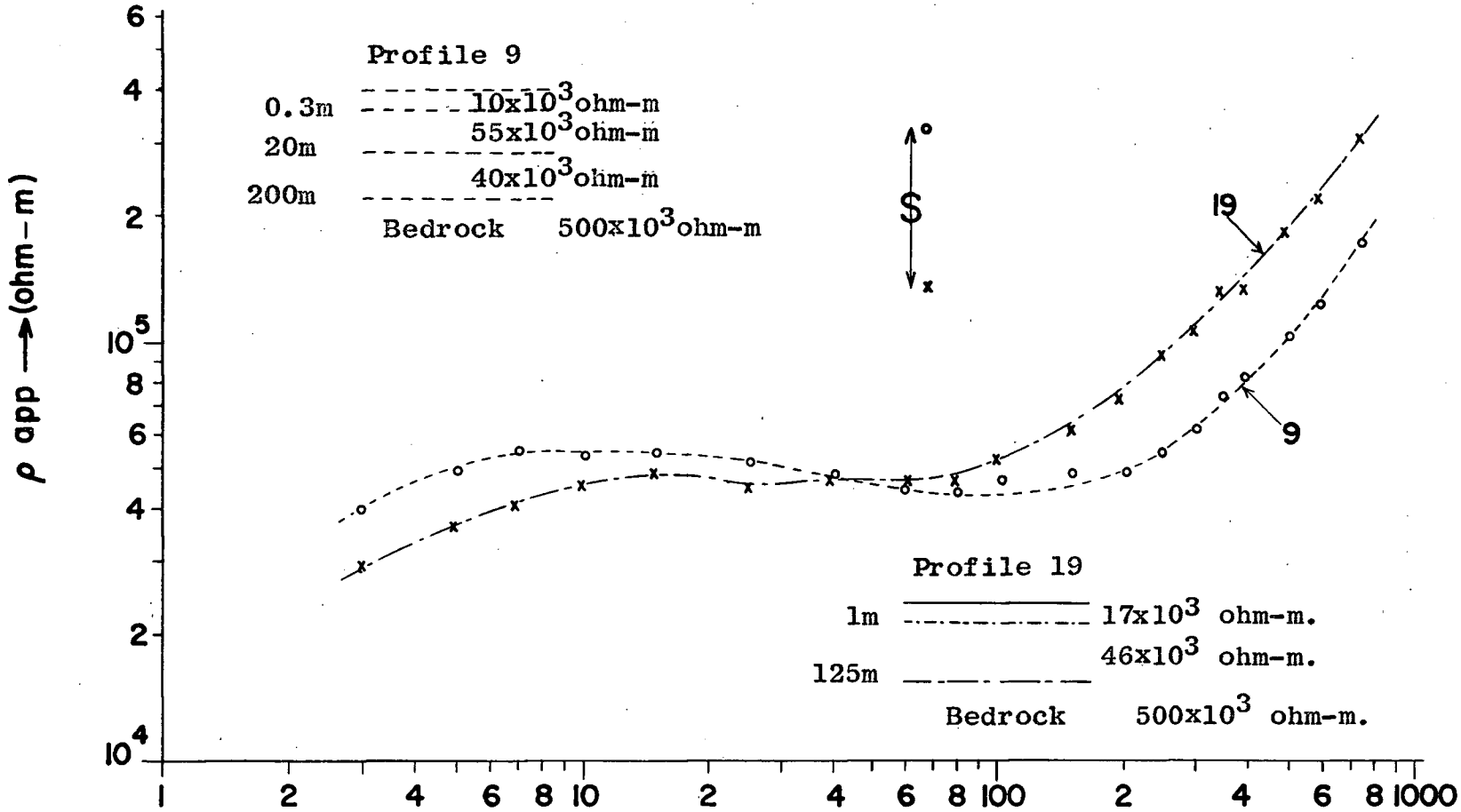

Figure 7. Sverdrup Glacier Profiles 9 and 19. (After K.Vogtli, Field Work of 1961) 19 29.6.61

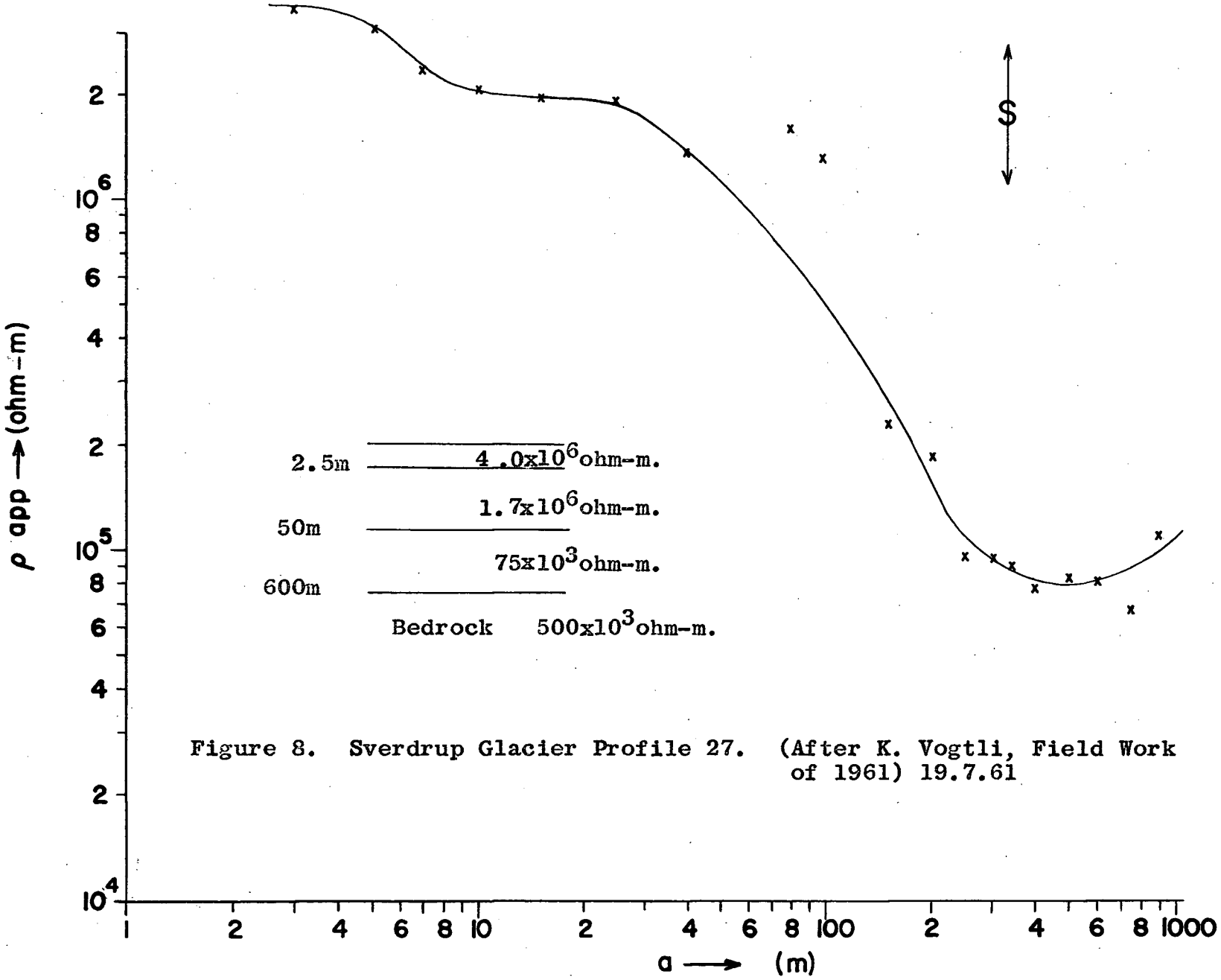

Figure 8. Sverdrup Glacier Profile 27. (After K. Vogtli, Field Work of 1961) 19.7.61

tation may be very inaccurate. The interpretations given with figures 7, 8 and 15 are by Dr. Vögtli.

1962

In 1962 resistivity measurements were taken at several locations (fig. 6) in both the accumulation and ablation zones. It was of particular interest to determine the effect of the firn layer on the apparent resistivity. It was to be expected that the gradual densification of the firn with depth would result in proportionately better conduction owing to the improved contact between grains. Hence the firn-ice transition of the apparent resistivity curve would not be expected to allow a two-layer interpretation.

At all points of the ice-cap some melting occurs, the amount depending primarily on the elevation but also on such factors as slope and surface albedo. Hence the firn is interspersed with ice-layers of a lower resistivity, and the apparent resistivity of the firn depends on the concentration of these layers.

Certain characteristics are common to nearly all the curves in the accumulation zone.

(i) There is a low resistivity layer in the top one to two meters. Pit studies (fig. 18) show this to be due to an unusually large concentration of ice layers, indicative of greater than usual melting in recent years.

(ii) There is a large shallow subsurface effect. This is the firn curve, the result of a layer of unconsolidated and poorly conducting snow accumulation which overlies the ice.

(iii) There is little or no bedrock effect. The maximum obtainable current at long electrode separations was insufficient to produce a voltage between the potential electrodes large enough to be distinguishable above the background noise. Readings under these circumstances were too erratic to properly define a terminal slope to the curve. Soundings of depths of ice greater than 800 meters require a greater current, a heavier cable, and possibly a commutating system on the potential electrodes.

That the firn-ice resistivity transition is a continuous process is obvious from the majority of the curves. In figures 9 to 14 the experimental curves are compared to two-layer standards to give an idea of the degree of anisotropy. When possible, the best fit with two or three-layer standard curves (see Appendix) for the firn-ice transition has been made and an interpretation given accordingly.

In figures 9 and 10 the best fit is obtained with two-layer standards. In figure 11 two-layer standards provide a reasonable fit to the plotted points but a better fit is obtained using three-layer standards having $\varrho_1 : \varrho_2 : \varrho_3 = 1:2/3:4/9$. Interpretations are given for both cases and it can be seen that there is considerable discrepancy.

In figure 12 the firn-ice transition will not match two-layer standards but a reasonable fit is obtained using three-layer standards having $\varrho_1 : \varrho_2 : \varrho_3 : = 1:3/7:9/49$.

In figure 13 two-layer standards provide a poor match, and suitable three-layer standards are not available. The curve in

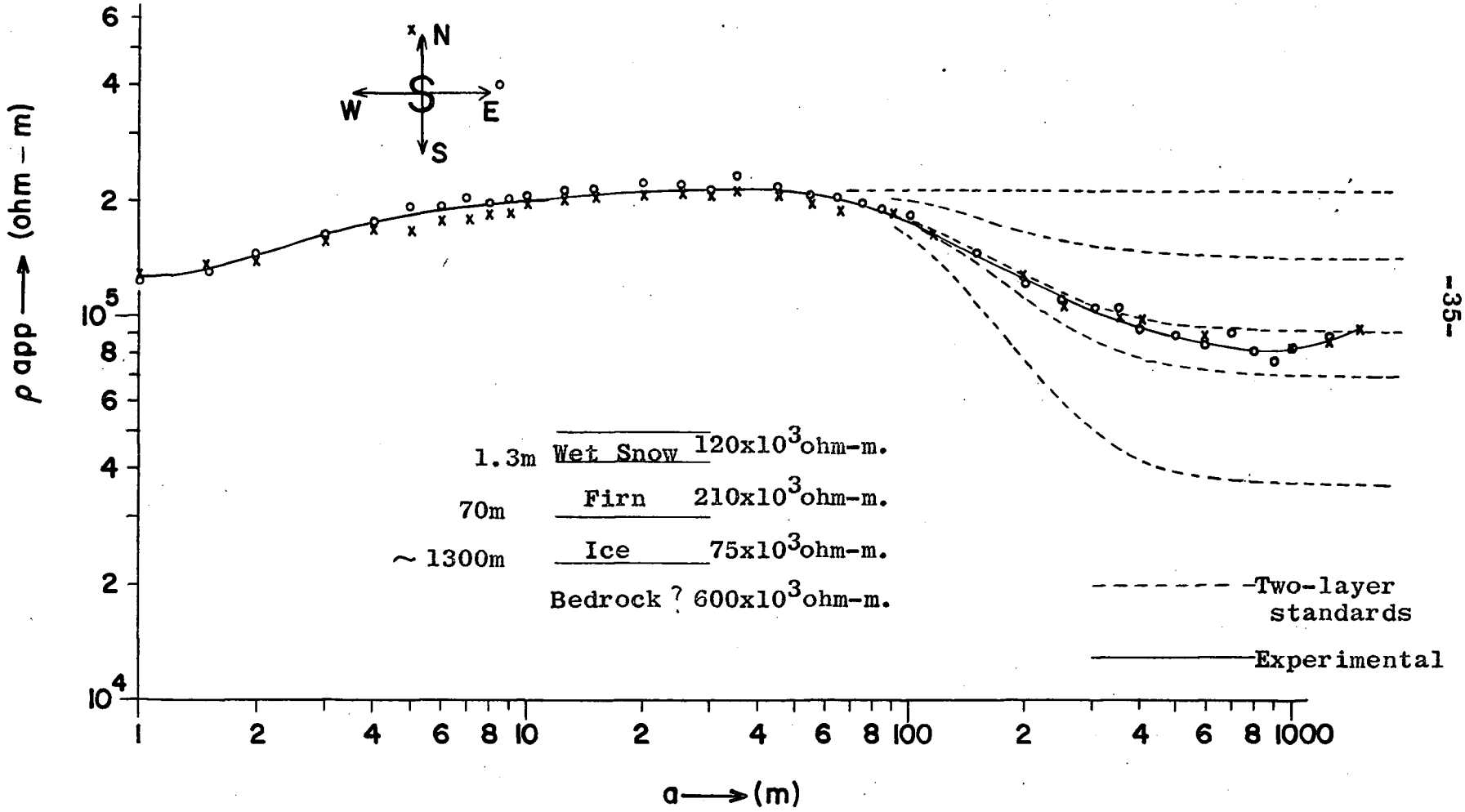

Figure 9. Ice-cap Profile 6. Elev. 1790m. 6-8.8.62

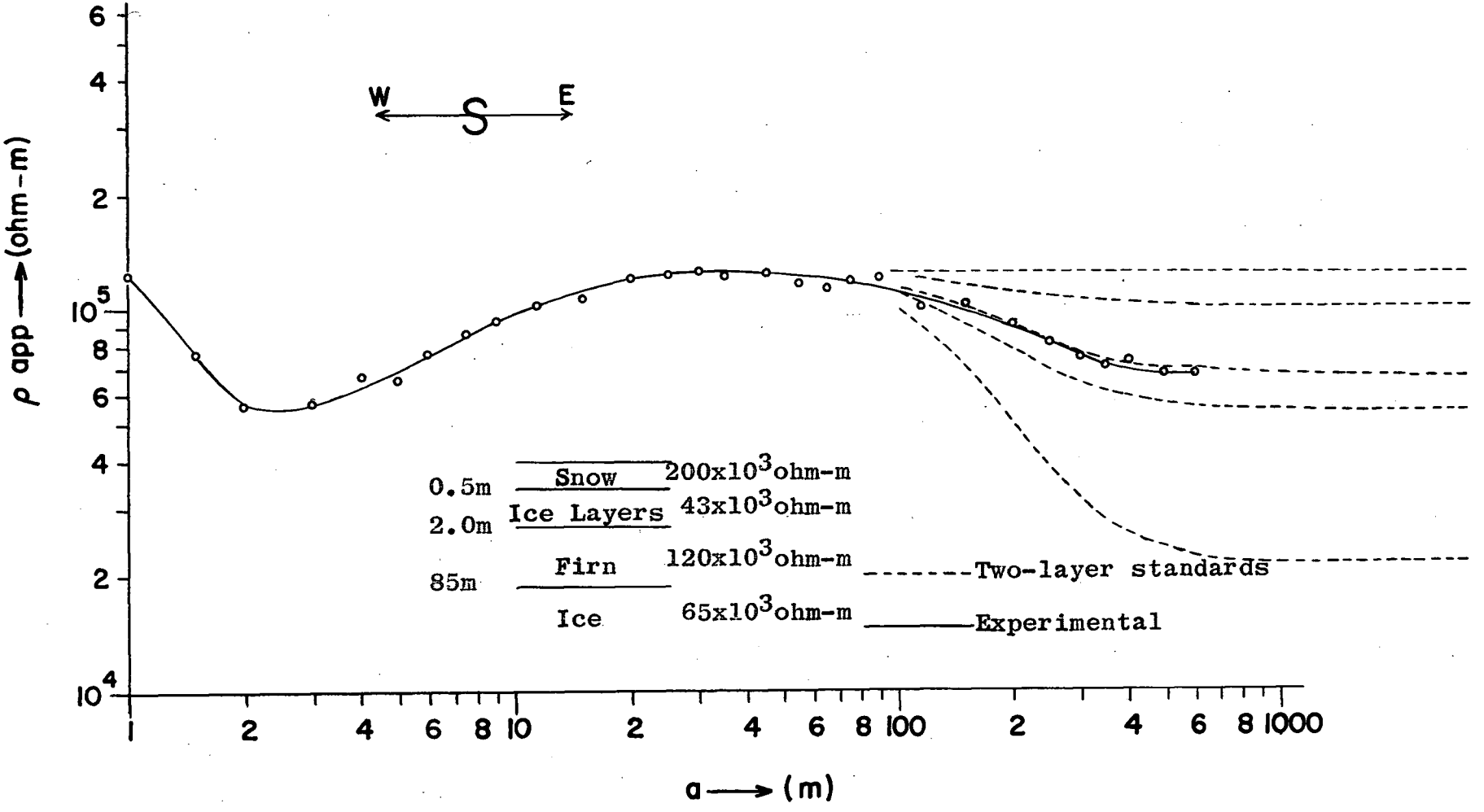

Figure 10. Ice-cap Profile 4. Elev 1598m. 10.8.62

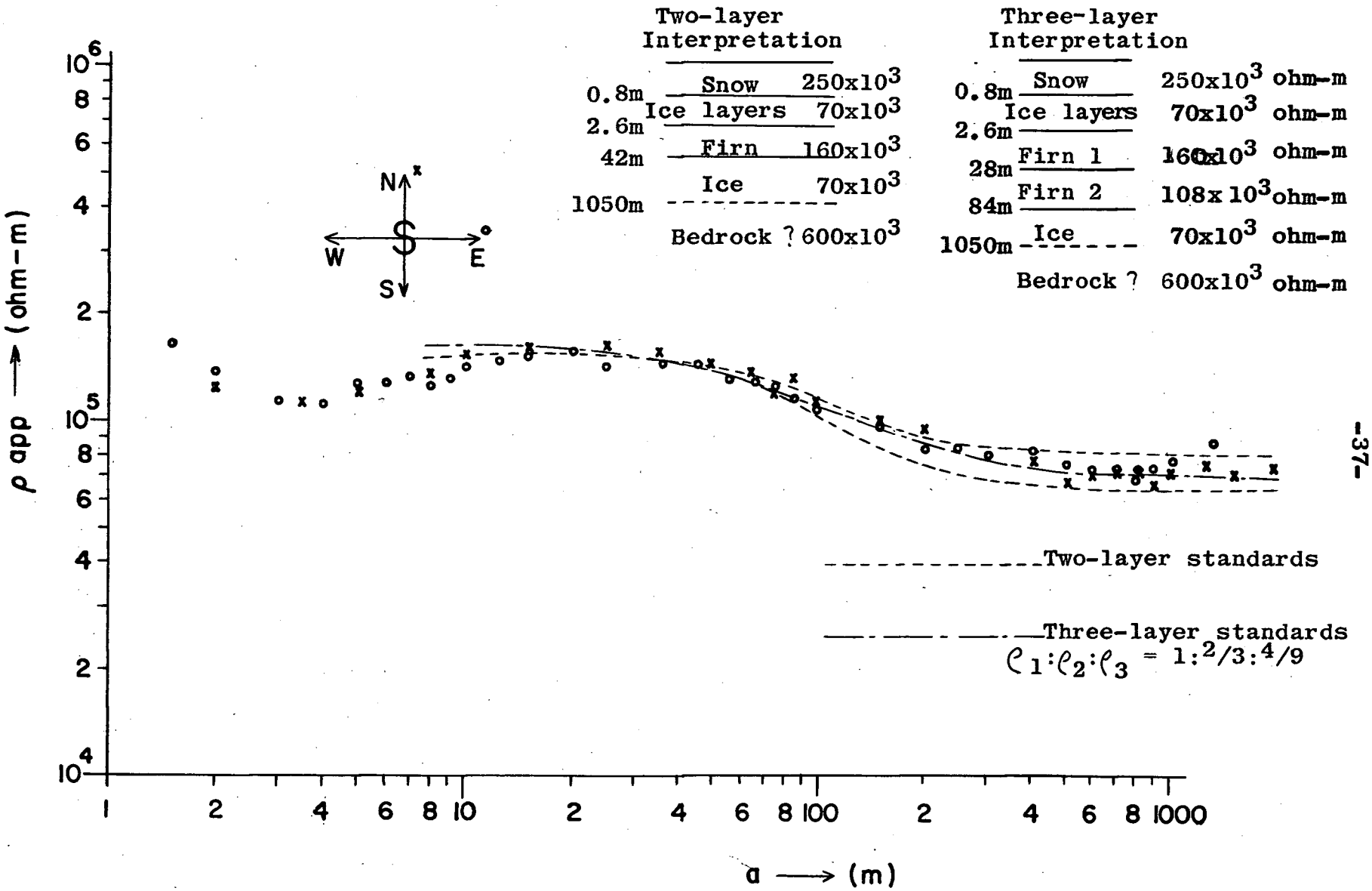

Figure 11. Ice-cap Profile 10. Elev. 1620m. 14-15.7.62

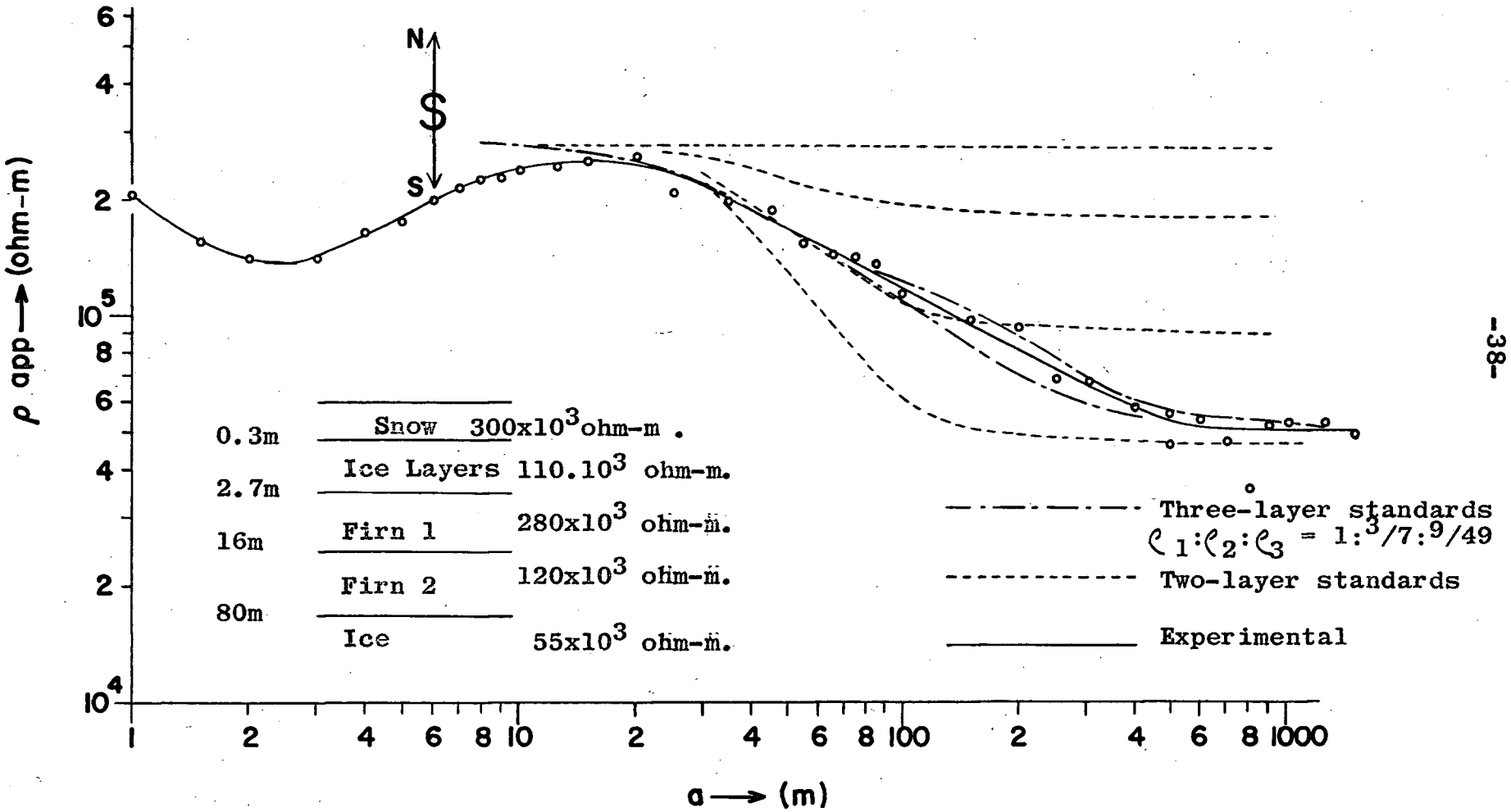

Figure 12. Ice-cap Profile 8. Elev. 1565m. 20.7.62

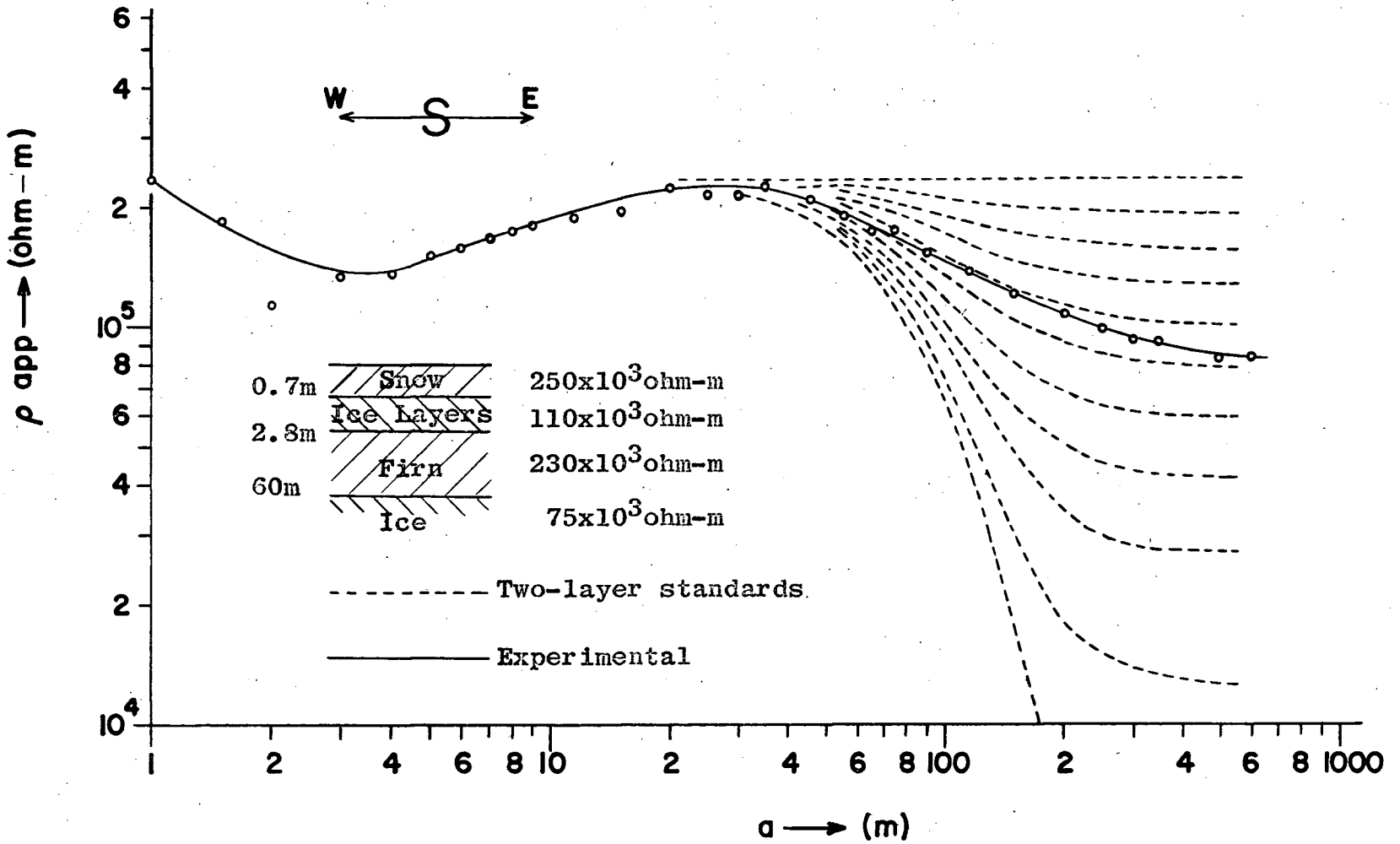

Figure 13. Ice-cap Profile 5. Elev. 1732m. 8.8.62

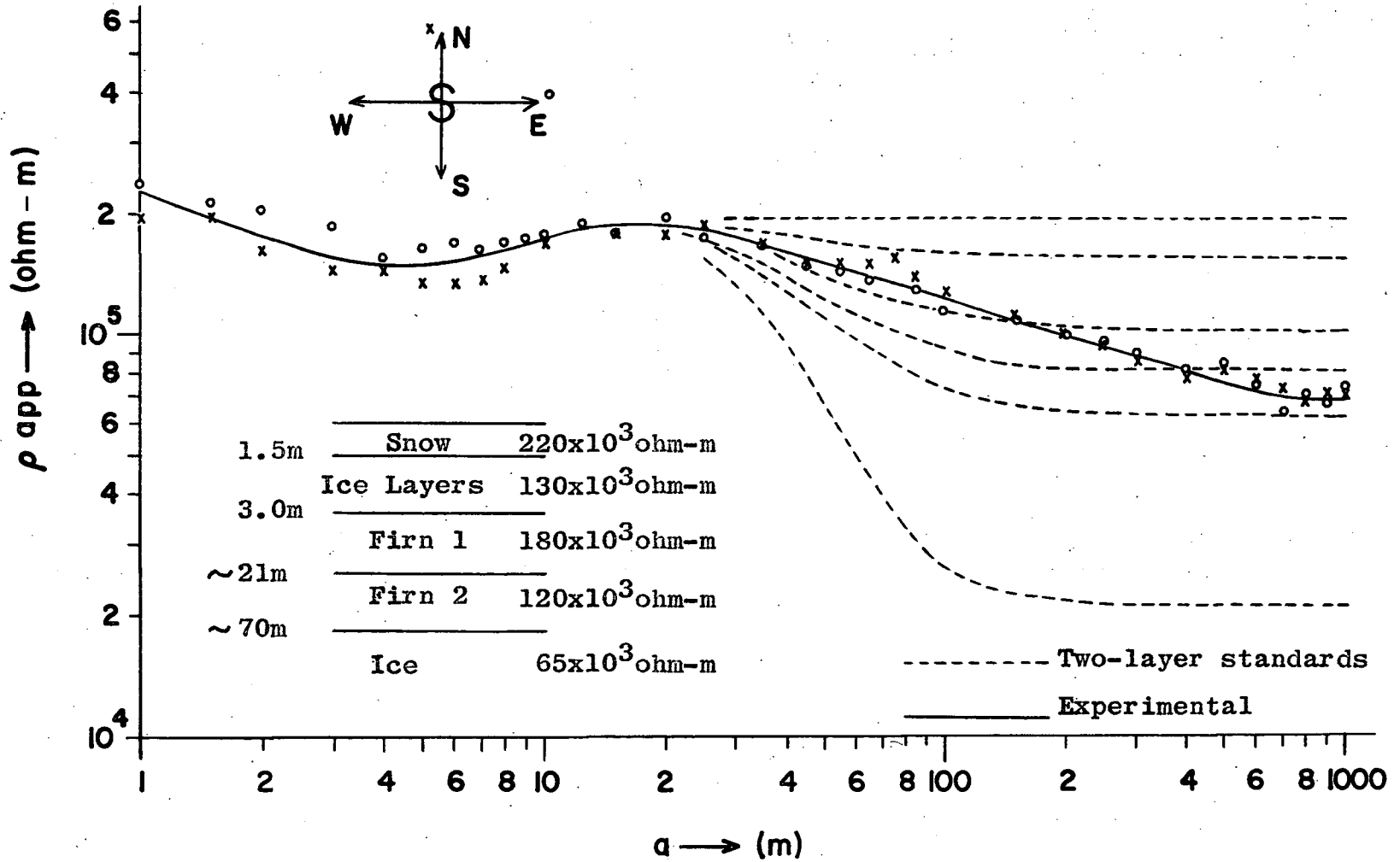

Figure 14. Ice-cap Profile 9. Elev. 1650m. 17-19.7.62

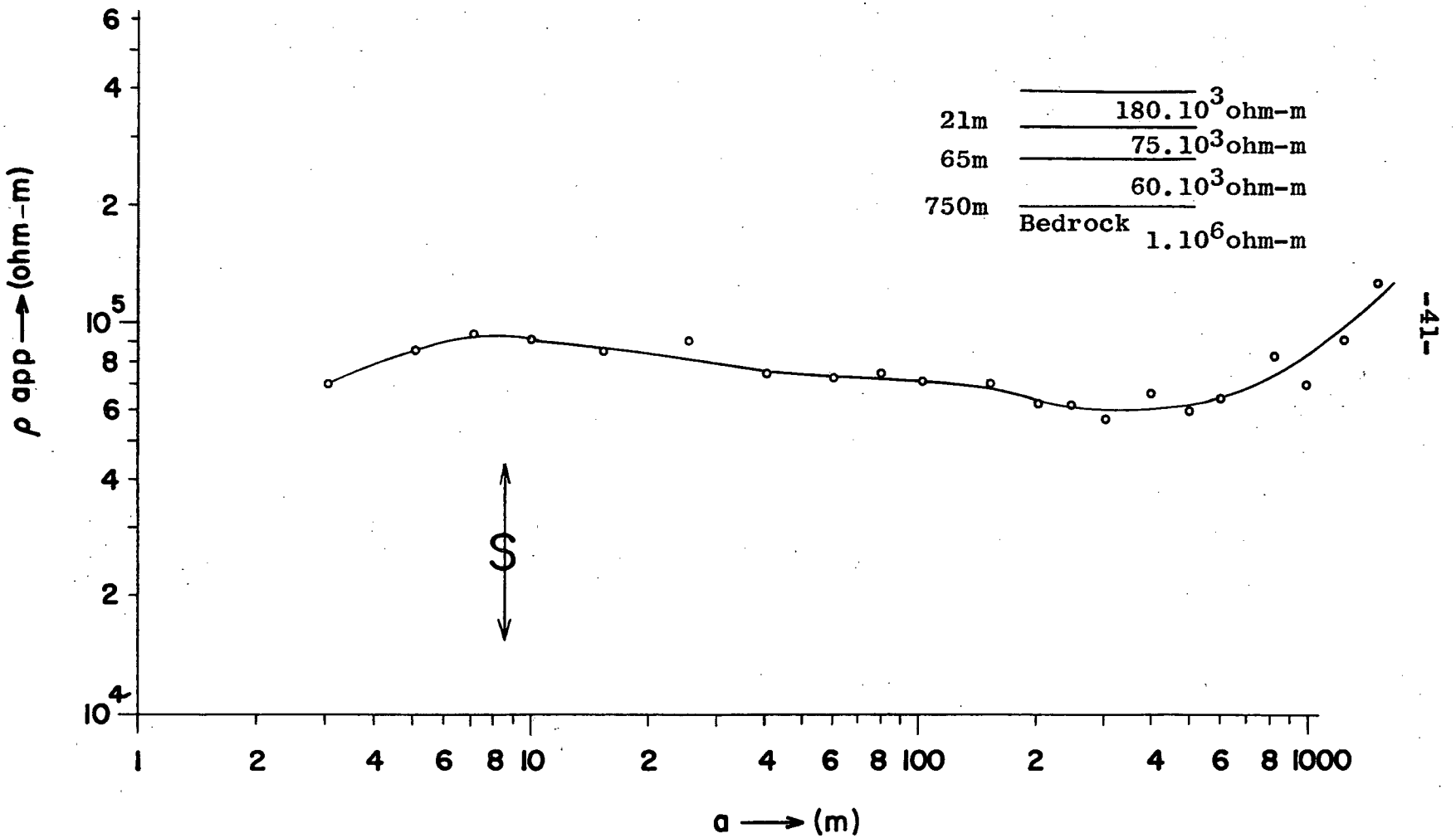

Figure 15. Ice-cap Profile 2. Elev. 1320m. 14.7.61.
(After K. Vogtli, field work of 1961).

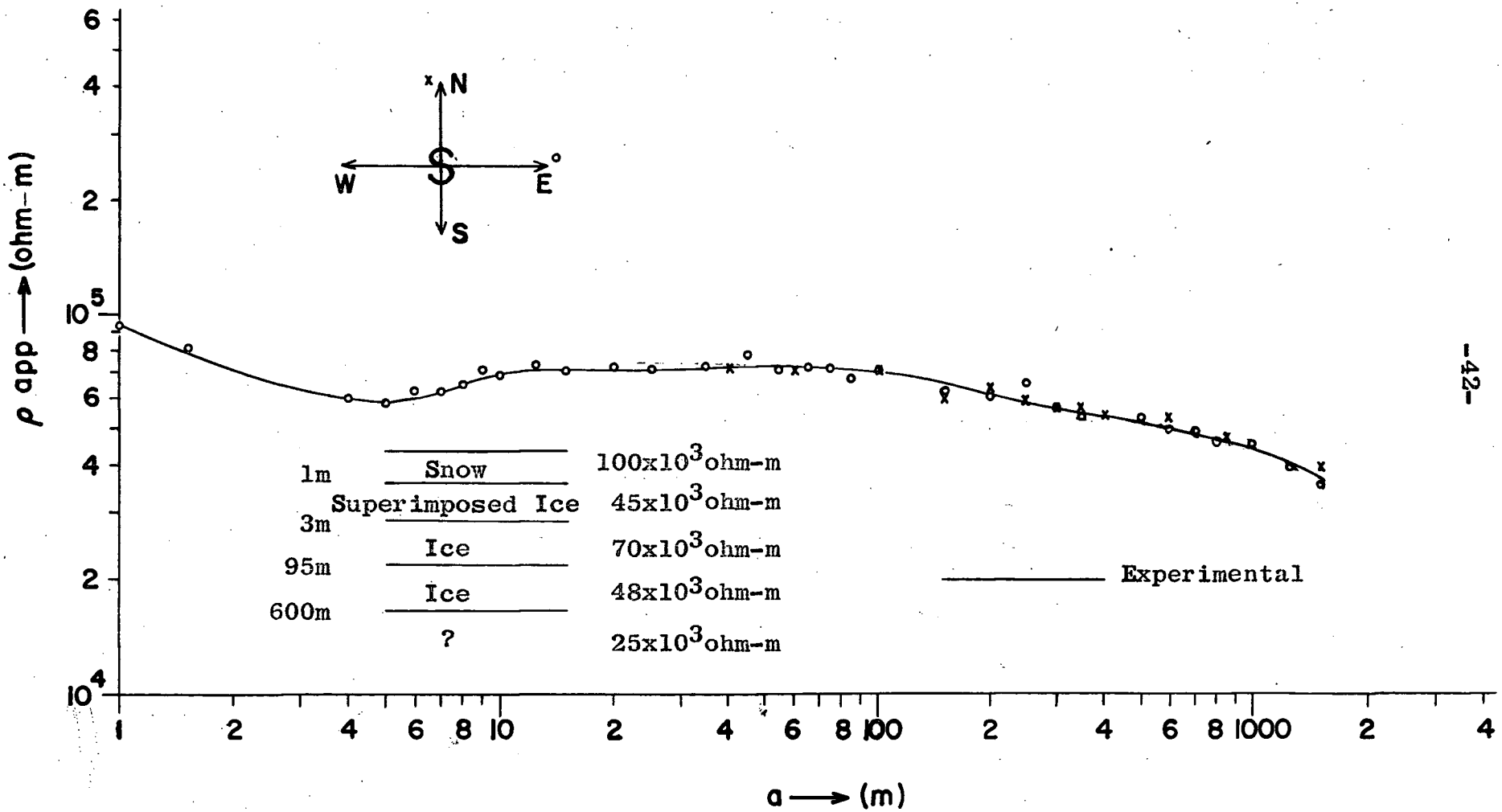

Figure 16. Ice-cap Profile 7. Elev. 1382m. 21.7.62
4.8.62

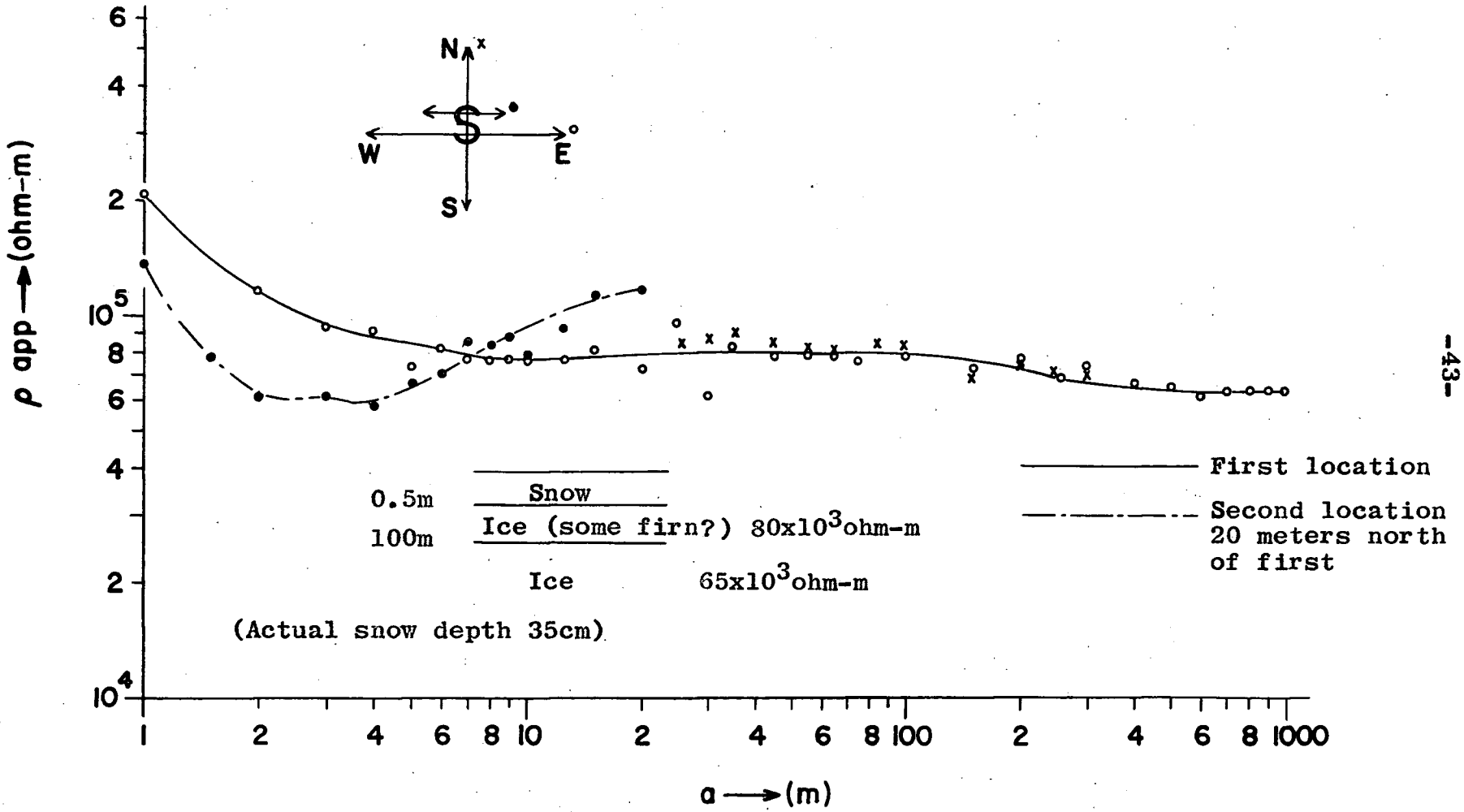

Figure 17. Ice-cap Profile 11. Elev. 1521m. 11-12.7.62

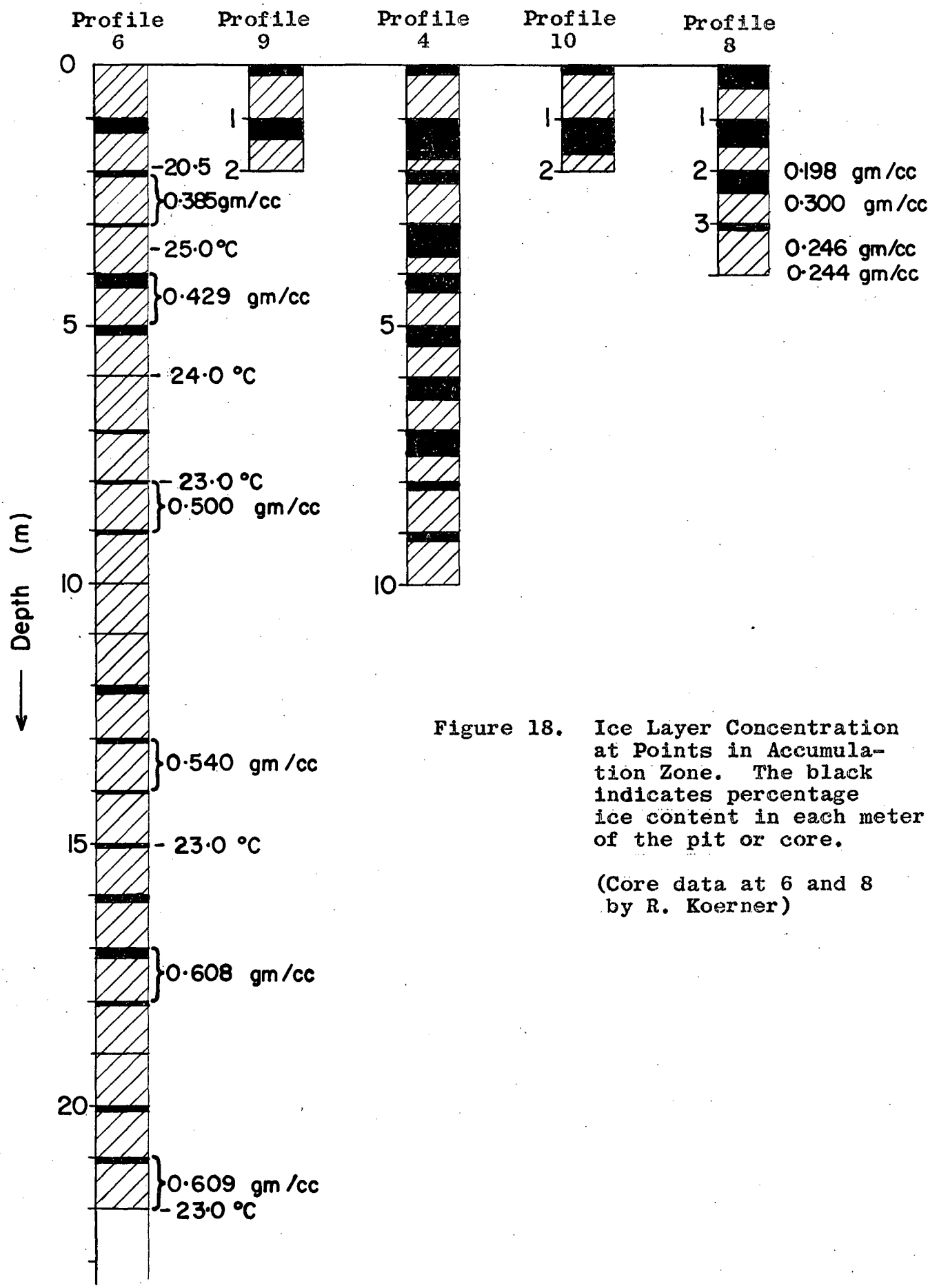

Figure 18. Ice Layer Concentration at Points in Accumulation Zone. The black indicates percentage ice content in each meter of the pit or core.

(Core data at 6 and 8 by R. Koerner)

figure 14 will not match two-layer standards and again there are no suitable three-layer standards available. Ice depth estimates are made in both cases by rough interpolation between the two sets of three-layer curves shown in the Appendix.

Figure 18 compares the relative concentration of ice-layers at several points in the accumulation zone at which profiles were measured. It is seen that the concentration at profile 4 is at least twice that at profile 6: this accounts for the difference in firn resistivity as shown in figures 10 and 9. It can be seen that the firn resistivities (upper layer in the interpretations) of profiles 4, 5, 6, 9, and 10 on the north slope of the ice-cap increase with elevation as predicted. However the firn resistivity at profile 8 on the southern slope is anonamously high in comparison. This is especially surprising since the southern slope receives more solar radiation. Since the ice layers are not evenly distributed over an area but rather occur as localized lenses, it can be assumed that profile 8 was measured at a point from which melt water was able to drain.

In figures 15 to 17 are shown curves from the ablation zone of the ice-cap. Notably absent is the firn curve. The curve in figure 16 has two notable features. First, it exhibits in common with profile 8 a low value of the bulk resistivity. There is a transition at 95 meters from 70.10^3 ohm-meters to a value of 50.10^3 ohm-meters more characteristic of the glacier. However, shorter profiles elsewhere indicated that this is not a widespread feature of the southern side of the ice-cap. Secondly, the downward slope at the end of the curve would indicate that the cap at this point

overlies a bed having a much higher conductivity than the Pre-Cambrian rocks underlying the glacier in the north. Direct readings on the sediments of the south coast showed them to have a resistivity quite similar to that of the Pre-Cambrian, although the summer thaw leaves a superficial layer of mud that is almost inpenetrable electrically. Weertman (1961) has suggested that the base of an ice cap in its central region may be at the melting point because the temperature gradient in the ice is insufficient to conduct away the geothermal heat and the heat produced by the sliding of the ice over its bed. If this was the case over a sedimentary bed it is conceivable that a layer of highly conducting mud would underlie the ice, producing a bedrock effect of the type seen in figure 16. While Weertman's assumptions and the present data need confirmation, a useful means of detecting such melting is suggested.

Profile 11 (fig. 17) was measured just below the acknowledged firn line in that area of the ice-cap. The high resistivity (80.10^3 ohm-meters) given for the first ice layer is probably due to small quantities of firn still present within the ice. A short profile (dotted line), measured 20 meters north of the original two for the purpose of testing equipment, has clearly been influenced by a local concentration of firn.

V. DISCUSSION OF THE CURVES

The effect of a dipping valley floor on interpretation.

It was assumed in the interpretation of the glacier profiles (figures 7 and 8) that the valley floor lay parallel to the surface of the glacier. Near the valley wall however the bed can be expected to dip quite sharply toward the center. Figure 19 shows the two-layer standard curves corresponding to three dip angles for a typical ice-rock resistivity contrast. The Wenner electrode configuration is assumed to be laid out in the direction of strike. It can be seen that for $\alpha = 22.5°$ a depth derived by matching horizontal layer standard curves ($\alpha = 0$) would be reasonably accurate but the resistivity given for the second layer would be too low. At greater angles of dip it becomes difficult to obtain a match with horizontal standard curves and a depth estimate would be very low. In practice then, profiles should be laid out parallel to the walls. The cross-sectional shape of the valley can be estimated knowing the width and the depth at the center; from this the observer must decide over what portion of the glacier's breadth it is meaningful to take readings. For an observer having independent information on the bedrock resistivity, the low resistivity given for the second layer in his interpretation must be diagnostic of a dipping bed.

The surface effect.

Figure 20 shows apparent resistivity variations over hourly periods for snow cover in the ablation zone of the ice-cap.

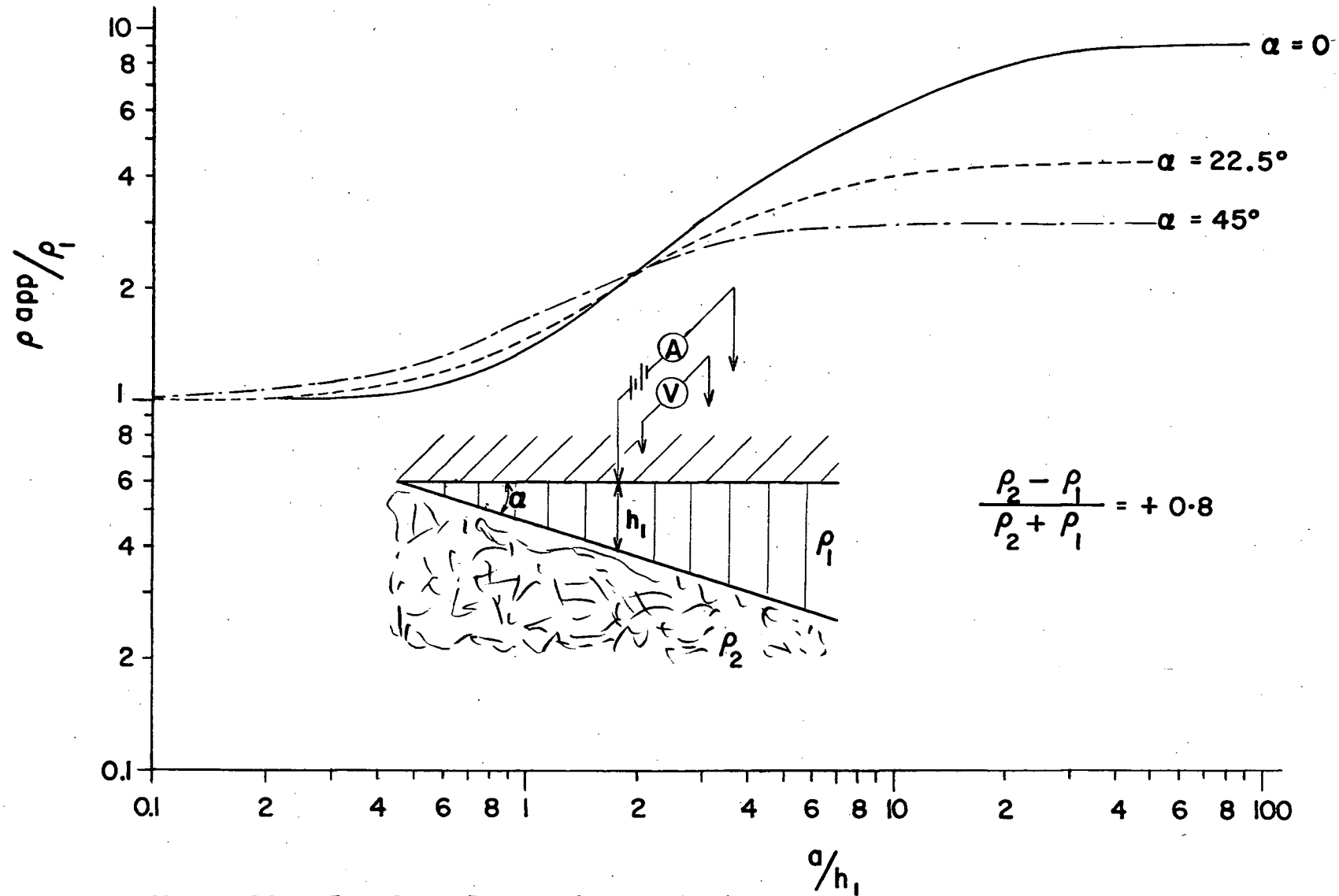

Figure 19. Standard Curves for a Dipping Bed. (After Unz, 1953, figures 11 and 13)

Readings were taken using four copper rods in a Wenner configuration. The dotted line envelope is made up of the two sets of readings having the maximum separation. The curves show the effects of solar radiation and increased air temperatures to extend to thirty or forty centimeters. Since the snow was well below its melting point the water content was low; when the water content is high, the snow resistivity in the first 20 centimeters can vary by a factor of ten during the 24 hour period. Figure 21 shows resistivity variations in the same locality over periods of a week and a month. It can be seen that the resistivity of the underlying ice has decreased with increasing temperature. Although the surface effect stems from the properties of a negligible fraction of the total ice thickness, it dominates a disproportionately large section of the apparent resistivity curve. On snow surfaces it can sometimes be eliminated by burying the electrodes.

The resistivity of firn.

An attempt was made to determine the firn resistivity as a function of depth in an 8 meter pit near profile 6 at the ice-cap summit. The difficulties of fixing the electrodes in the vertical wall and of making electrical contact with the cold firn resulted in considerable scattering of the readings, but an average of many such measurements indicated that the resistivity of firn layers from two to eight meters in the pit lay in the range 3-4 . 10^5 ohm-meters.

It is significant that in all the accumulation zone profiles

the resistivity of the firn layer (i.e. firn plus ice layers) stays constant to a depth of at least 15 meters, despite the fact that the greatest rate of densification occurs in that interval. At the ice-cap summit, where little melting takes place, the firn curve is a plateau extending to 50 or 60 meters. Unfortunately the snow densification process at all points of the ice-cap is interfered with by meltwater. In the dry-snow facies where there is no melting (Benson, 1959, fig. 17), it is possible that the electrical conducting properties of firn at a given temperature are not affected by densification until a critical loading is reached, at which point the individual grains fuse and their contact resistance vanishes.

Deep drill cores have not yet been taken on the Devon Island ice-cap. Figure 22 shows a density-vs-depth graph for a point just below the dry-snow facies at 2140 m. on the Greenland ice-cap. The density value of 0.82 gm/cc, at which the previously interconnecting air spaces in the firn are cut off to form bubbles, occurs at approximately 80 meters. Considering the elevation difference, the firn depth of 70 meters given in profile 6 with a two-layer interpretation is not unreasonable.

The shallow subsurface effect in ice.

The high apparent resistivities often found in the top ten to twenty meters of ice can be attributed in part to low ice densities. The average of 54 density measurements taken from three to ten meters at the Ice-cap Station was 0.887 gm/cc with standard deviation 0.018 gm/cc. Three other possible influencing

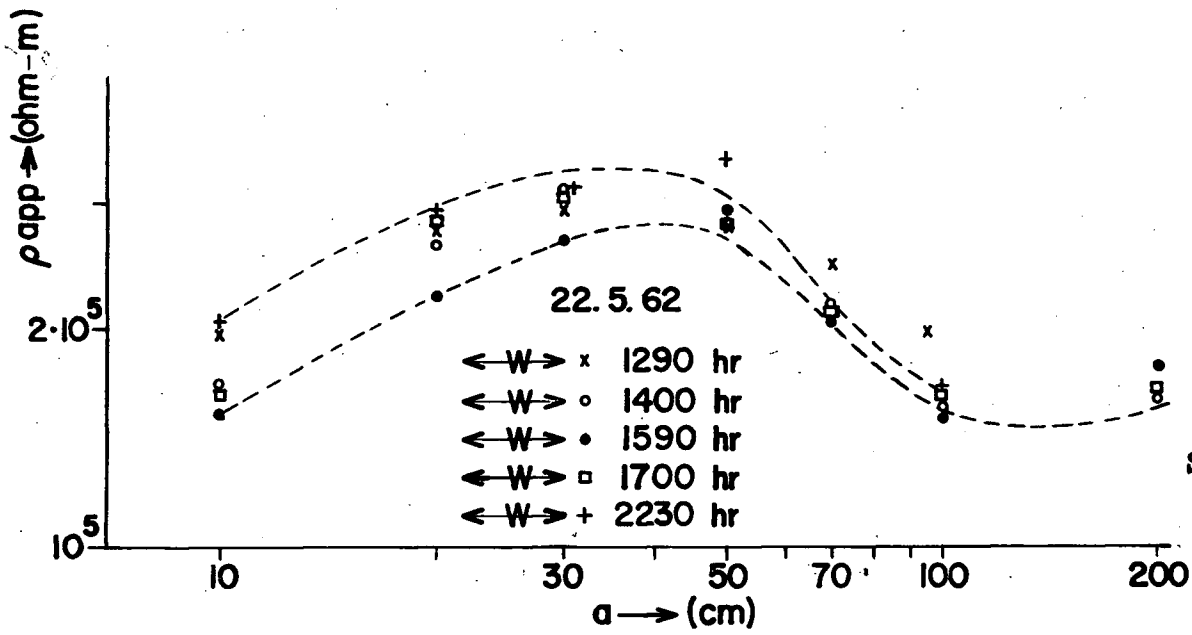

Time of day (hours)

Depth below surface (cm)	1200	1500	1800	2100	2400
0	12·2	11·2	2·5	−7·4	−11·2
8	2·2	5·0	5·2	2·9	+0·1
15	0·4	2·7	3·2	2·1	0·0
30	−1·4	0·4	1·1	0·7	−0·7
79	−4·8	−4·8	−4·8	−4·8	−4·8

Snow Temperatures (°F)

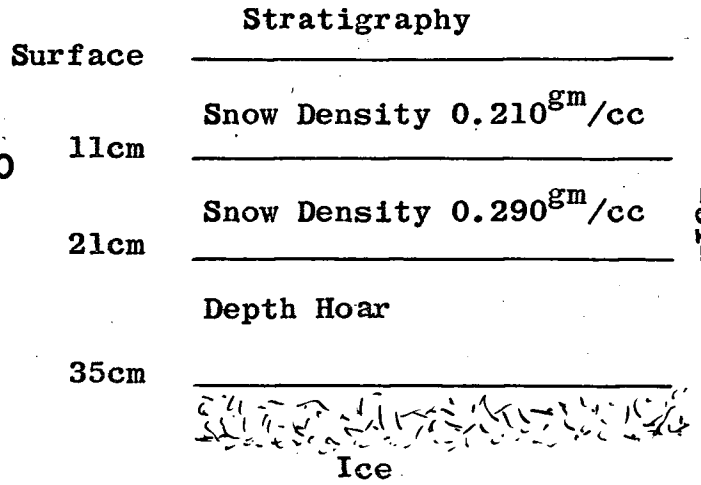

Figure 20. Profiles on Snow Cover - Ablation Zone. Hourly variations in the apparent resistivity.

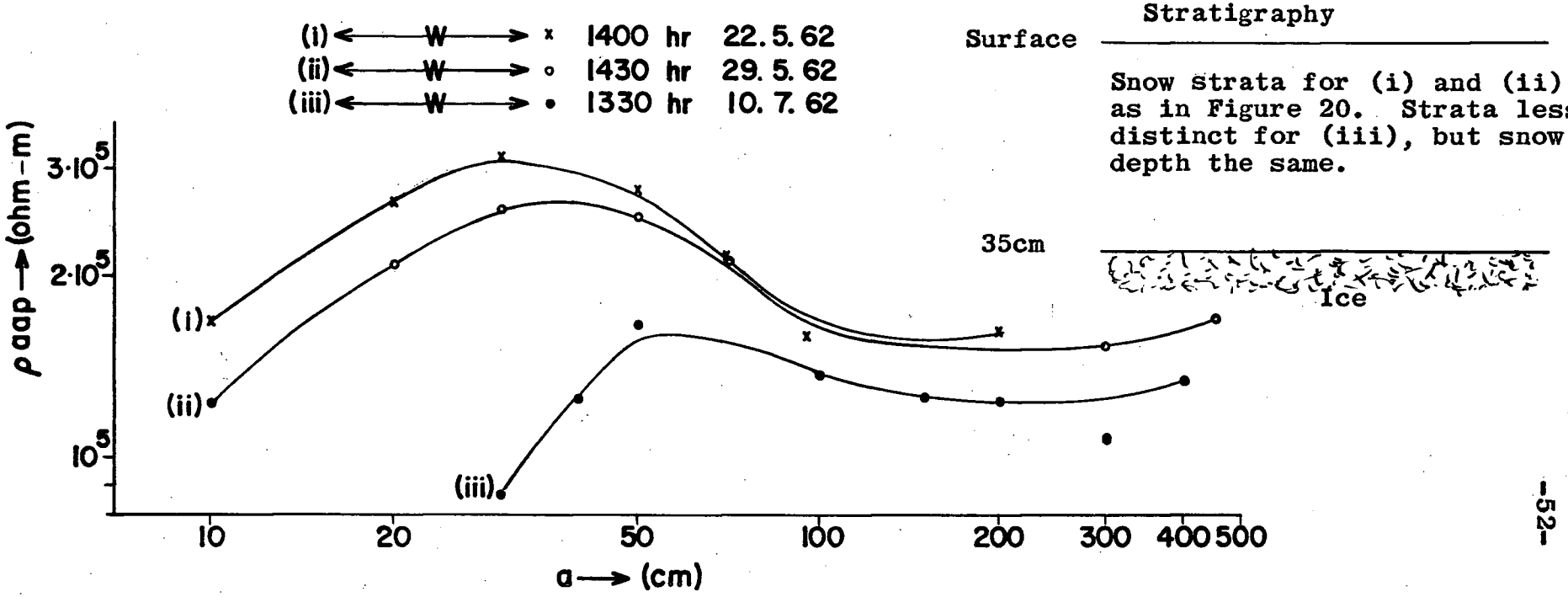

Figure 21. Profiles on Snow Cover-Ablation zone. Variations in the apparent resistivity over periods of one week and one month. (Ice-cap Station).

Depth below surface (cm)	1500 hrs. 22.5.62	1500 hrs. 29.5.62	1200 hrs. 10.7.62
0	11·2	21·5	0
8	5·0	17·9	29·5
15	2·7	14·7	25·9
30	0·4	1·6	15·4
84	−4·8	−3·1	10·3

Snow Temperatures (°F)

factors were investigated.

(i) Internal stress. The very high resistivity observed in figure 8 occurred on a ridge of ice about ten meters wide and one meter high running parallel to the wall for six kilometers on the upper part of the Sverdrup Glacier. Subsequent measurements showed that similar shallow subsurface effects occurred frequently but not consistently at other points of the ridge. On a second ridge, much higher than the first but extending only a few hundred meters, similar near surface resistivities were again found. This ridge was believed to be caused by the pressure of a small tributary glacier entering the main stream. Running across the ridge in a zig-zag fashion was a series of cracks as shown in figure 23(b). Apparent resistivities were measured at a number of points across the ridge using a Wenner configuration with electrode separations of three meters and ten meters. The values obtained are plotted in figure 23(a). The cracks themselves were filled with water at that time of year and hence were not directly responsible for the anomalous resistivity. From the correlation of the apparent resistivity with the crack pattern it was tentatively assumed that the stresses involved affected in some manner the conduction mechanism, probably through variations in crystal size or orientation. However an alternative explanation is that the ridges contain air tunnels, since it is not uncommon for melt streams to flow beneath the surface.

(ii) Temperature. Two short profiles taken two months apart in the ablation zone of the ice-cap are shown together with subsurface temperatures in figure 24. Each curve is a composite

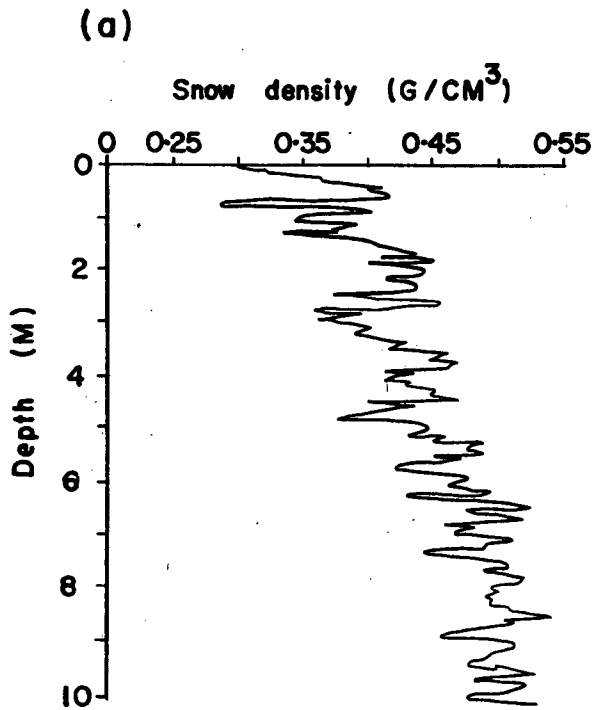

Snow Density Profile at 77°N, 56°W

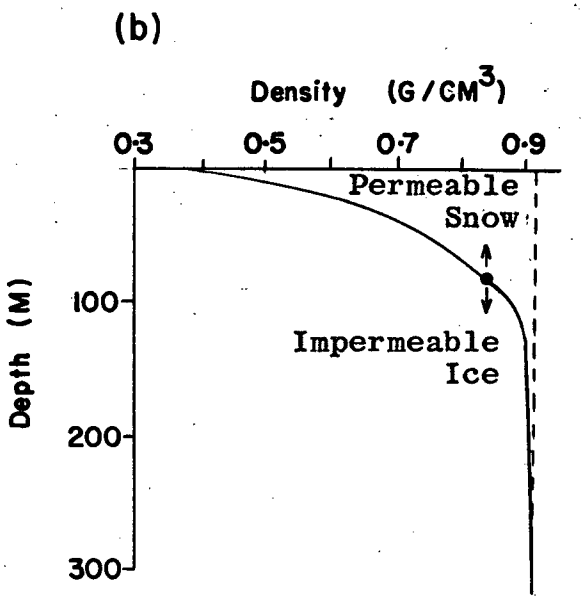

Depth Density curve at 77°N, 56°W.

Figure 22. Density-vs-Depth at Upper Limit of Percolation Facies, Greenland Ice-cap. (After Bader, 1958, figures 3 and 4).

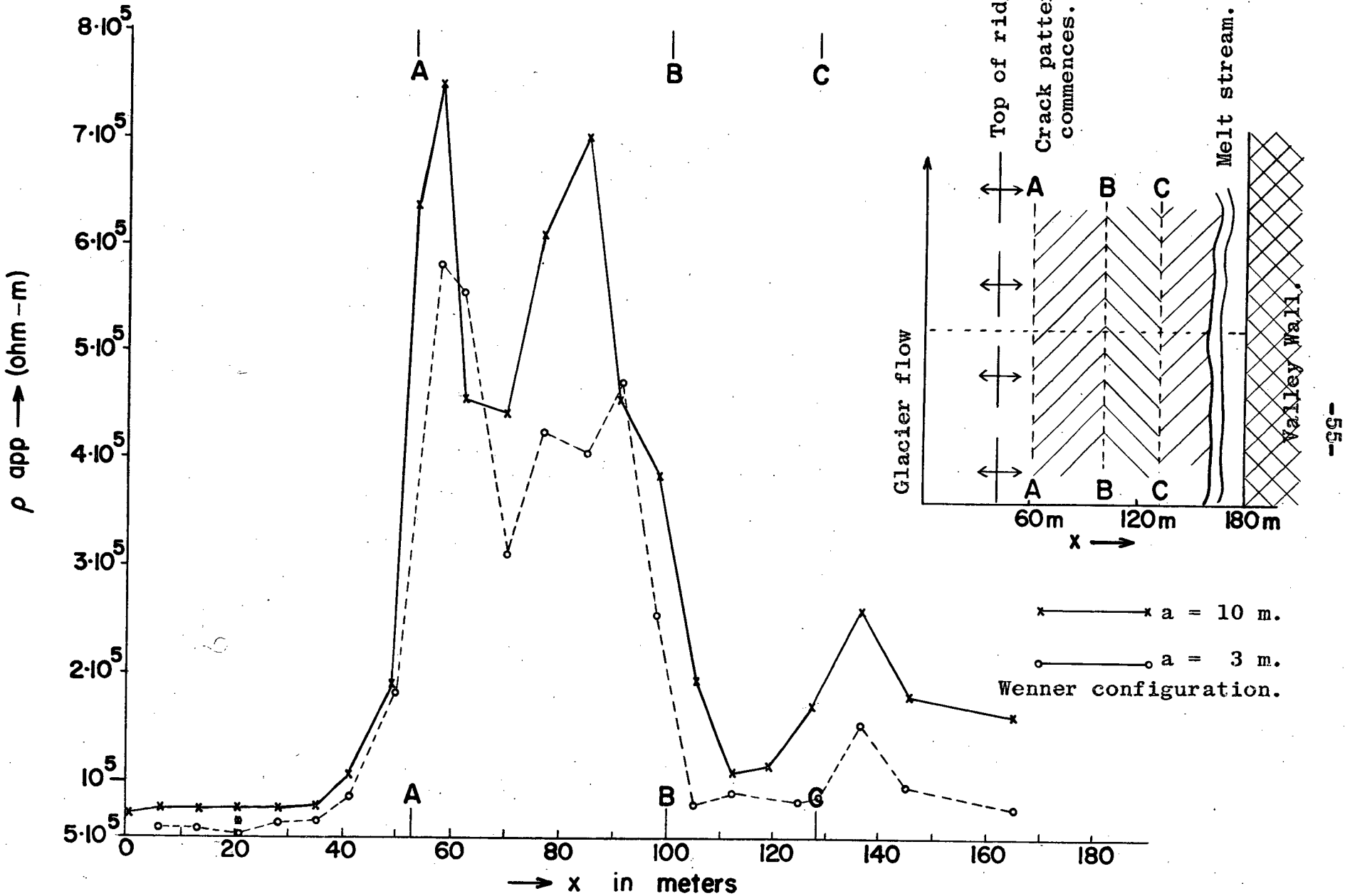

Figure 23. Anomalous Resistivity on Ridge of Sverdrup Glacier. 12.8.61

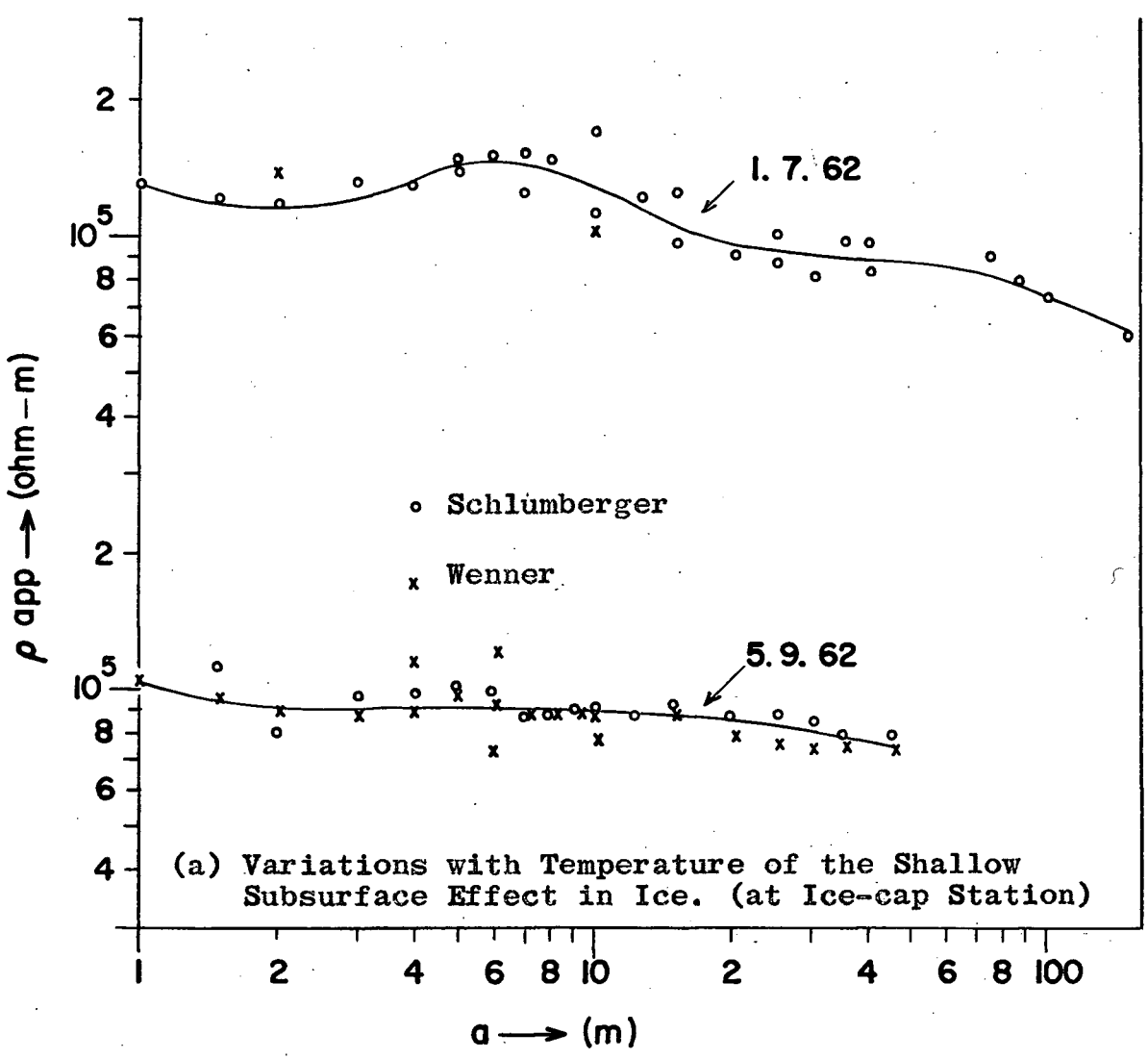

(a) Variations with Temperature of the Shallow Subsurface Effect in Ice. (at Ice-cap Station)

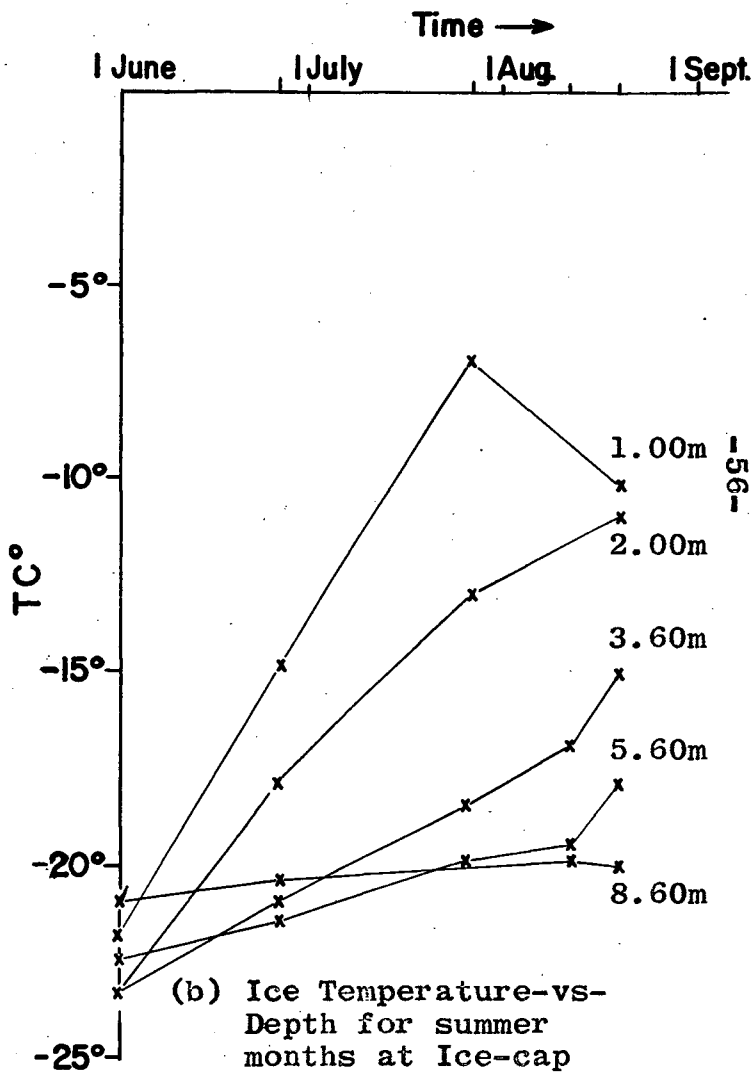

(b) Ice Temperature-vs-Depth for summer months at Ice-cap Station.

Figure 24.

of at least three sets of measurements in the area. Surface conditions were similar in both cases. Although ice temperatures were not available for September, they should fall at about the same rate that they rose and the temperatures from two to eight meters would be considerably higher in September than they were in July. The magnitude of the shallow subsurface effect is seen to fall accordingly. In figures 21 and 24 increases of 5°C to 9°C in ice temperature decrease the ice resistance by 20 to 40 percent. However, although the shallow subsurface effect in this case in influenced by temperature, it can not originally stem from temperature differences since the ice at -12°C (fig. 22) still has a resistivity well above the bulk resistivities of the glacier and ice-cap.

(iii) Detrital material. The effect of moraine material in the ice is to lower the resistivity considerably. It is thus not responsible for the shallow subsurface effects. An attempt to make use of this property in finding the slope at which the material forming the shear-plane moraines is brought up from the bottom was unsuccessful because of equipment trouble and a shortage of time. This is another potentially useful application of resistivity methods.

Low densities or variations in the crystal structure are thus seen as the most probable causes of the shallow subsurface effect in ice. When correlated with detailed glaciological information this effect could yield useful qualitative evidence for the near surface properties of the ice.

The bulk resistivity.

There is a definite tendency for the bulk resistivity of the ice to increase in going from the glacier snout to the top of the ice-cap. Profiles 9 and 19 (fig. 7) show values between 40 and 50 . 10^3 ohm-meters, while the ice-cap values range from 60 to 80 ohm-meters. It is improbable that there is much variation of density at depth within the ice sheet. However, crystal size and temperature are known to increase during the outward flow of ice and both phenomena could result in increased conductivity. The crystals grow through fusion of one to another in the flow process (Sharp, 1960, p. 61). Bader (1961, p. 13) estimates that the energy of flow is converted into heat at a rate of 2.34 . 10^3 cal. per gram per meter drop in elevation, corresponding to a temperature increase of 0.47°C per 100 meters or about 10°C over 2000 meters. That these values are at least approximately correct was born out by temperature measurements at depth in Greenland. If this is the case, the bulk resistivity variation coincides in order of magnitude with the observed resistivity-temperature variations discussed in the previous section.

VI. CONCLUSIONS

This study has attempted to present a background of material for persons interested in applying resistivity methods to the problems of glaciology. The data is in many cases incomplete; not only are more results required from different geographic localities but independent information (i.e. seismic soundings, deep drill holes) is required for purposes of comparison.

The resistivity method provides a means of sounding up to 800 meters of ice using lightweight equipment that is inexpensive and extremely simple to operate. Using three men, a sounding of 800 meters can be completed within three hours. Unlike a.c. and pulsed d.c. methods, the unshielded cables can be laid directly on the ice, and with suitable precautions the equipment may be used under all except the worst surface and meteorological conditions.

The accuracy of depth determinations can not be expected to exceed fifteen percent. Depths of ice greater than 800 meters would require slightly heavier equipment; however, if mechanical transportation is available for all phases of the measurement, the sounding of 2000 meters of ice should not present an undue problem.

The method can locate regions of relatively high or low resistance within the ice. If these variations can be definitely correlated with variations in temperature and crystal structure they may provide useful information - possibly of the type described by Borovinski (1960). In addition, the method can detect the

presence of old snow and firn within the ice and can give an idea of the ice layer concentration beneath points in the accumulation zone.

The following applications have also been suggested:

(i) The method may provide a good estimate of the depth of firn in the accumulation zone of an ice mass, especially in the dry-snow facies. Useful information might also be obtained on the densification process in the firn.

(ii) It could provide evidence for basal melting of an ice-cap, by detecting either the relatively warm ice or possibly a layer of highly conducting mud overlying the bedrock.

(iii) It could be used to detect crevasses and underground melt stream tunnels.

(iv) It could be used to trace detrital material within the ice, notably in the case of shear-plane moraines.

The comparatively low resistivity of the Arctic ice masses investigated to date is thought to be the result of impurity content or structural peculiarities. It has been suggested that chemical analysis together with resistivity measurements in the accumulation zones and on refrozen melt samples should determine the issue.

REFERENCES

1. Auty, R.P. and Cole, R.H. "Dielectric Properties of Ice and Solid D_2O." Journal of Chemical Physics, 20, 1952, pp. 1309-1314.

2. Bader, Henri. The Greenland Ice Sheet. U.S. Army Cold Regions Research and Engineering Laboratory Publication 1-B2, Sept. 1961.

3. Benson, C. S. Physical Investigations on the Snow and Firn of Northwest Greenland 1952, 1953, and 1954. Research Report 26, U.S. Army Snow Ice and Permafrost Research Establishment, 1959.

4. Borovinski, B.A. "On the Question of the Research of the Glaciers by the Method of the Electrical Prospect". Publication No. 54 of The International Association of Scientific Hydrology - General Assembly of Helsinki, 1960. pp. 492-499.

5. Carpenter, E.W. "Some Notes Concerning the Wenner Configuration". Geophysical Prospecting, 3, 1955, pp. 388-402.

6. Eigen, M. and deMaeyer, L. "Self Dissociation and Protonic Charge Transport in Water and Ice". Proceedings of the Royal Society of London, 247 (Series A), 1958, pp. 505-533.

7. Keller, G.V. and Frischknecht, F.C. "Electrical Resistivity Studies on the Athabaska Glacier, Alberta, Canada". Journal of Research (N.B.S.), 64D, 1960, pp. 439-448.

8. Kuroiwa, D. "The Dielectric Properties of Snow". Publication No. 39, of The International Association of Scientific Hydrology - General Assembly of Rome, 1953, pp. 52-63.

9. La Compagnie Générale de Géophysique. "Abaques de Sondage Electrique". Geophysical Prospecting, 3 (supplement 3), 1955.

10. Lee, F.W. "A New Depth Meter for Ice and Snow". Bulletin No. 23 of The International Association of Scientific Hydrology, 1936, pp. 761-771.

11. Lefeure, C., Albertinoli, M.M.P., Bauer, A., Blum, A., Cagniard, L., Fournier, H. "Mésures Electrique et Telluriques Sur le Grand Glacier d'Aletsch". Annales de Géophysique, 13, 1957, pp. 54-68.

12. Maeda, K. "Apparent Resistivity for Dipping Beds". Geophysics, 20, 1955, pp. 123-139.

13. Review of the Properties of Snow and Ice, ed. H.T. Mantis. SIPRE Report No. 4, July 1951.

14. Mikhailov, I.G. "The Determination of Glacier Thickness Using the Electrical Resistivity Method". Izvestiia Akademii Nauk SSSR (Seriia Geograficheskaia i Geofizicheskaia), No. 4-5, 1939, pp. 417-420. SIPRE Abstract.

15. Mooney, H.M., and Wetzel, W.W., The Potentials about a Point Electrode and Apparent Resistivity Curves for a Two-, Three-, and Four-Layer Earth. University of Minnesota Press, Minneapolis, 1956.

16. Muskat, M. and Evinger, H.H. "Current Penetration in Direct Current Prospecting". Geophysics, 6, 1941, pp. 397-427.

17. Queille-Lefeure, C., Bauer, M.M. and Girard. "Premier Essai de Mésure Electrique d'un Glacier (Glacier de Saint Sorlin)." Annales de Géophysique, 15, 1959, pp. 564-567.

18. Roman, I. "Electrical Resistivity of Ice and Snow". Bulletin No. 23 of the International Association of Scientific Hydrology, 1936. pp. 483-493.

19. Shimada, H. "Electrical Resistance of Snow". SIPRE Translation No. 31 (Seppyo, Vol. 3, 1941), 1954.

20. Siksna, R. "Conduction of Electricity Through Ice and Snow" (Parts I and II). Arkiv For Fysik, 11, 1957, pp. 495-529.

21. Sharp, R.P. Glaciers. Oregon State System of Higher Education (Condon Lectures), University of Oregon Press, 1960.

22. Stefanesco, S., Schlumberger, C. and Schlumberger, M. "Sur la Distribution Electrique Potentielle autour d'une Prise de Terre Ponctuelle dans un Terrain a Couches Horizontal Homogenes et Isotropes." Le Journal de Physique et le Radium, Series 7, Vol. 1, 1930, pp. 132-140.

23. Unz, M. "Apparent Resistivity Curves for Dipping Beds." Geophysics, 18, 1953, pp. 116-137.

24. Vögtli, K. "Die Bestimmung des Specifischen Widerstandes von Schlechtleitenden Geologischen Korpern." Rapport No. 14103, Direction Generale des PTT; Laboratoire de Reserche et d'Essais, 9.7.57.

25. Vögtli, K. "Aufnahme und Auswertung geoelectrischer Profile." Rapport No. 14104, Direction Generale des PTT; Laboratoire de Recherches et d'Essais, 19.7.57.

26. Watt, A.D. and Maxwell, E.L. "Measured Electrical Properties of Snow and Glacial Ice". Journal of Research (N.B.S.), 64D, 1960, pp. 357-361.

27. Weertman, J. "Mechanism for the Formation of Inner Moraines Found near the Edge of Cold Ice Caps and Ice Sheets". Journal of Glaciology, 3, 1961, pp. 965-978.

APPENDIX

Figures (i) and (ii) show standard curves for the two and three-layer situations depicted.

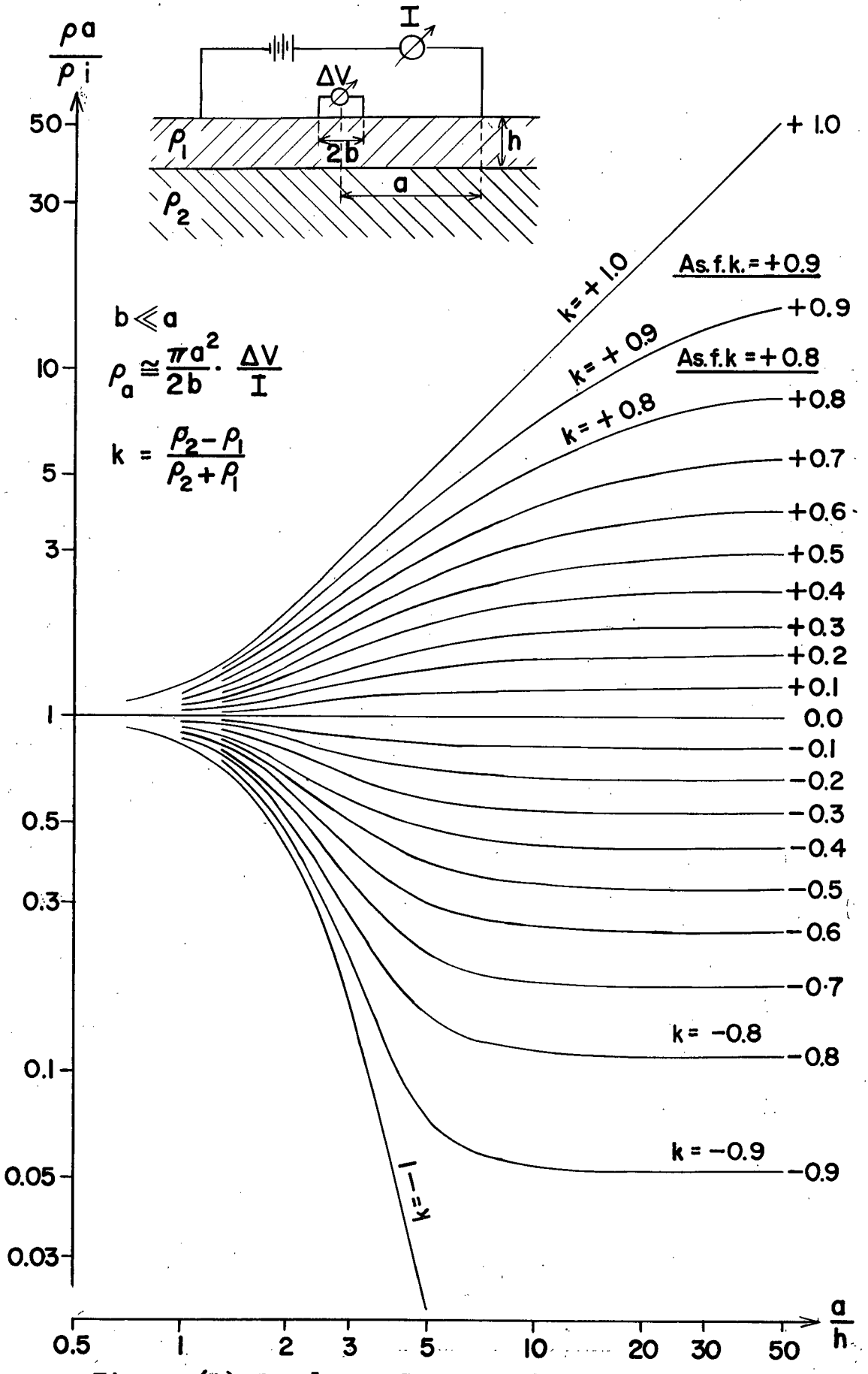

Figure (i) Two-layer Standard Curves

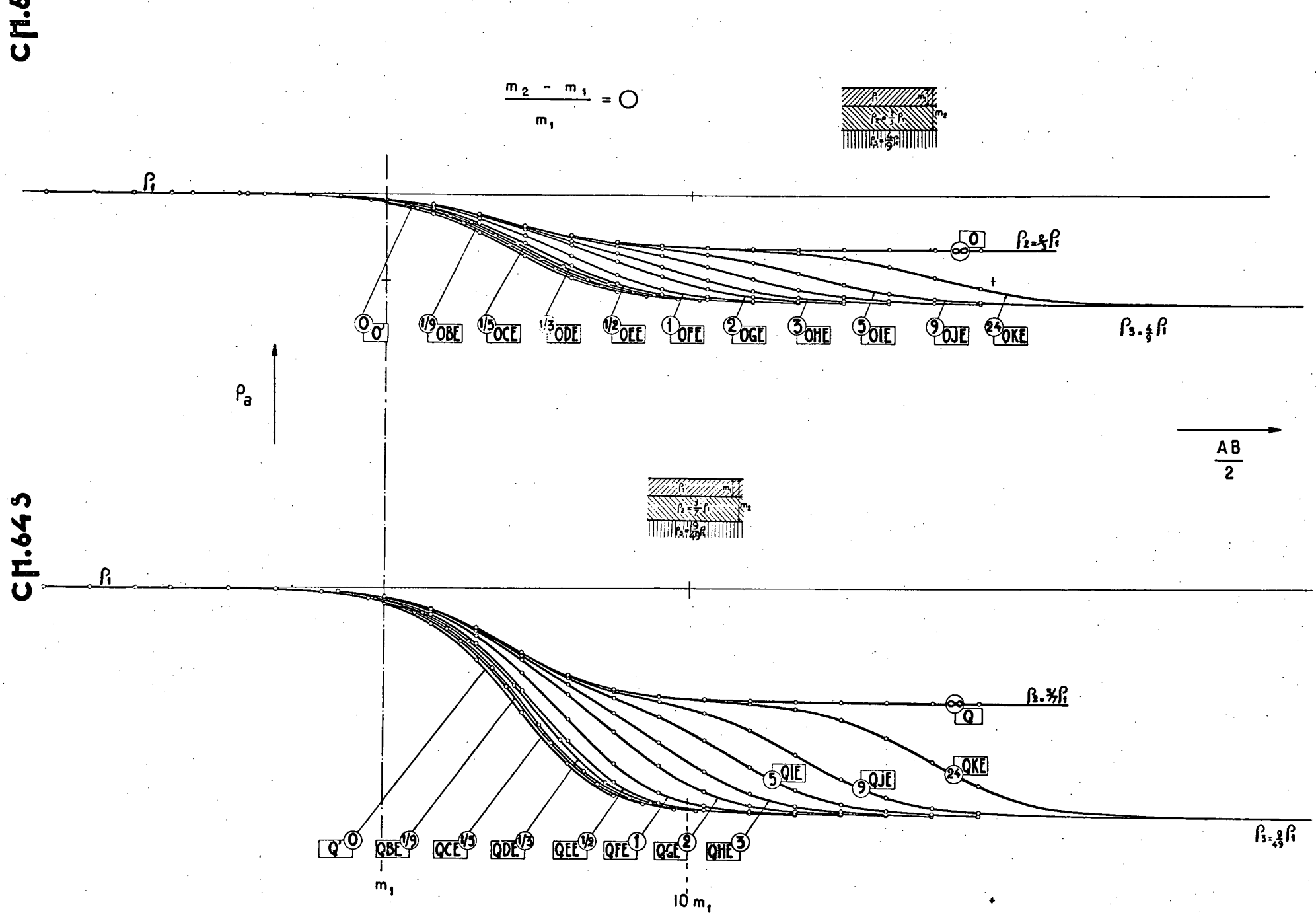

Figure (ii) Three-layer Standard Curves. (Calculated by La Compagnie Générale de Geophysique).

Calculé par la Compagnie Générale de Géophysique Paris . 1933-1936.